TECTONICS, VOL. 4, NO. 7, PAGES 739-780, DECEMBER 1985

p. de 40

QUATERNARY NORMAL AND REVERSE FAULTING AND THE STATE OF STRESS IN THE CENTRAL ANDES OF SOUTH PERU

Michel Sébrier,[1] Jacques Louis Mercier,[1] François Mégard,[2] Gérard Laubacher,[3] and Evelyne Carey-Gailhardis[1]

Abstract. Field studies in the Andes of southern Peru show that in the High Andes and Pacific Lowlands, Quaternary and Recent faults are normal. This extensional tectonics postdates compressional deformations of Pliocene-early Quaternary age. In the sub-Andes the observed deformations are compressional; they affect early Quaternary deposits. Some of the faults separate Quaternary deposits from the bedrock and thus are clearly of tectonic origin and not landslide effects. Striations on the fault planes indicate N-S trending extension in the High Andes and Pacific Lowlands. The total amount of crustal stretching is small, probably of the order of 1% during the last 1-2 m.y. In the sub-Andes, folds and faults affecting Neogene and early Quaternary deposits result from N-S shortening. Nevertheless, it is supposed that this N-S shortening is of early Quaternary age. The present-day compression probably strikes E-W, judging from focal mechanisms in the sub-Andes of central Peru, southern Bolivia, and northwest Argentina. Data from structural analysis of faults and from earthquake focal mechanisms allow us to surmise the state of stress in the Andes of southern Peru. The High Andes and Pacific Lowlands, subjected to N-S trending extension, are bounded by two zones of E-W trending compression: the sub-Andes to the east, and the contact between the convergent Nazca and South America plates to the west. In our model the maximum horizontal compressive stress trajectory σ Hmax is roughly parallel with the E-W convergence between the two plates; σ Hmax corresponds to σ 1, in the sub-Andes and to σ 2 in the High Andes. The latter situation is caused by the elevated mass of the High Andes, where σ zz (the vertical stress) is inferred to be σ 1. Thus the third principal stress axis, being orthogonal to the other two axes, is oriented N-S, allowing extension to occur in that direction. On the other hand, in the sub-Andes σ zz is σ 3, and horizontal E-W shortening occurs. The state of stress in the Andean continental crust above the 30° dipping slab appears to be different from that in the Andes of Central Peru situated above the flat subducting segment. In this region, compressional deformations affect a wider part of the Cordillera.

[1]Laboratoire de Géologie Dynamique Interne, Université Paris-Sud, Orsay, France.
[2]Centre Géologique et Géophysique, Université des Sciences et Techniques du Languedoc, Montpellier, France.
[3]Office de la Recherche Scientifique et Technique d'Outre-Mer, Paris, France.

Paper number 5T0550.
0278-7407/85/005T-0550$10.00

INTRODUCTION

Two main types of subduction zones have been distinguished by Uyeda and Kanamori (1979): the Mariana type with extensional tectonics and back arc spreading and the Chilean or Andean type with compressional tectonics and no back-arc spreading. However, it is already known that normal faults have been reported in the Central Andes (Heim, 1949; Silgado, 1951; Audebaud et al., 1973; Aubouin et al., 1973). In the Andes of Peru and Bolivia, Quaternary extensional normal faults have been analyzed (Dalmayrac, 1974; Lavenu, 1978; Soulas, 1978; Lavenu and Ballivian, 1980; Yonekura et al., 1979; Sébrier et al., 1980b, 1982) and extension has been considered as the typical state of stress of the Altiplano during Quaternary and Recent times (Mercier, 1981). Some authors have considered this extensional tectonics as a quite negligible, purely superficial, and local phenomenon (Allmendiger et al., 1983; Jordan et al., 1983). Nakamura and Uyeda (1980) have suggested some physical processes which can be responsible for extensional tectonics along subduction zones, such as landward decrease of σ Hmax, gravitational body forces, etc. Recently, this extensional tectonics has been interpreted as an effect of the highly compensated topography (Cross and Pilger, 1982; Suarez et al., 1983), and a two-dimensional model has been presented (Dalmayrac and Molnar, 1981; Froidevaux and Isacks, 1984).

In the Andes of Peru, Bolivia and northernmost Chile, two recent and active tectonic domains have been separated in relation to the dip of the subducted slab (Stauder, 1975; Barazangi and Isacks, 1976, 1979; Mégard and Philip, 1976), their common boundary lying at about 14° S (Hasegawa and Sacks, 1981; Grange, 1983; Grange et al., 1984a). North of this latitude, the slab dips at about 30° below the trench inner slope, the shelf, and the coast. Farther east, it flattens and is almost horizontal under the Andes. In this region, E-W Quaternary compression is observed in a wide part of the Andes (Sébrier et al., 1982; Blanc et al., 1983; Blanc, 1984), but extension is present along the coast (Soulas, 1978; Sébrier and Macharé, 1980; Macharé, 1981) and in the western part of the High Andes, particularly in the Cordillera Blanca (Dalmayrac, 1974; Yonekura et al., 1979; Dalmayrac and Molnar, 1981; Sébrier et al., 1982). South of 14° S latitude, the slab dips steeply, and Quaternary extension is widespread in the Andes. This extensional tectonics is evidenced mainly by E-W trending recent and active normal faults both in the Pacific Lowlands and the High Andes. In the latter, extension is associated with Recent volcanic activity. Compressional faulting is restricted to the lowlands of the sub-Andes which bound the High Andes to the NE.

Structural analysis of the normal faults indicates a N-S trending tensional tectonics which postdates early Quaternary compressional movements. The few crustal earthquakes analyzed by Grange (1983) in the Western Cordillera also indicate N-S tension. Relations between seismicity and superficial deformations are more complicated along the faulted boundary between the coast and the Western Cordillera. In the present paper we describe all the Quaternary faults that we have observed in south Peru. Since seismicity is generally low, we first used Landsat imagery to search the most conspicuous fault zones of south Peru. Then we focused our field work on the faulted Quaternary basins which are associated with the major Quaternary fault zones and offer possibilities to decipher Recent fault movements. Further we surveyed southern Peru along the road network using aerial photographs in order to discover and study in the field other fault zones not easily seen on Landsat imagery. Field studies begin in 1978. Quaternary faults are of primary interest because of the scarcity of focal mechanisms in that part of the Andean Cordillera.

EXTENSIONAL TECTONICS IN THE HIGH ANDES

The Huambo-Cabana Conde Active Fault Zone, Western Cordillera

Geometry of the faults. In the Western Cordillera, about 100 km north of Arequipa (Figure 1), lava plateaus lie at a mean elevation of 4 km between the villages of Huambo and Cabana Conde (Figure 1, point 8). They are crossed by the major, nearly E-W trending Trigal and Solarpampa faults and by some other minor faults nearly parallel to them (Figures 2a and 2b). The faulted area is about 28 km long in the E-W direction and 10 km wide from north to south. This faulted zone extends to the

west into the Uncapampa plateau located 7.5 km north of Huambo. In the area east of Cabana Conde some short faults of the same system crosscut the volcanic flows vented from the Ampato volcanic center located 10 km farther to the south. West of 72°W longitude, the mean trend of the faults is N82°E, with extreme values of N77°E and N90°E. Toward the east, the faults curve to a N105°E-N120°E direction in the area of Cabana Conde. The Trigal fault is about 10 km long, and the Solarpampa fault is 12 km long. The length of the minor faults range between 1 and 5 km. Some minor faults branch out from the major ones; generally, throws decrease away from the main fault. All these faults are easily identified both in the field (Figure 2a) and on aerial photographs (Figure 2b) thanks to well-developed scarps that are usally 5-10 m high but reach locally 30 m for the major faults. Most of the scarps are south facing, this being opposite to the drainage, causing sagponds to form where the faults cross the few intermittent streams draining the plateaus. Most of these sagponds are filled with sediments.

According to surface observations, most of the faults dip southward with values ranging between 60° and 70°, but the crude columnar jointing in the lavas at the surface makes precise observations difficult. Some slickensides were measured along the roadcut on the right bank of Quebrada Trigal (Figures 3 and 4, site 8). At its western end, this fault has a local N114°E trend and a 62° south dip. At its eastern end, values of N108°E with 74° south dip and N94°E with 84° south dip were measured along two branches of the fault. Some north dipping faults have been also observed in particular a plurikilometric fault crossing the southern part of the lava plateau 2 km north of lake Mucurca has a north facing scarp 5-10 m high. Along all the faults, dip-slip movement always prevails over strike-slip, so that no lateral displacements of the streams have been observed and all the striations that we measured have pitches ranging between 48° and 88° (Figure 4, site 8) with a clear maximum around 80°. The general southward dip of these normal faults is a strong argument against a huge landslide faulting due to the at least 2000-m-deep incision of the Colca River located north of the lava plateaus (Figure 2a).

Age of faulting. Morphological arguments favor a very recent age for the last movements along these faults: (1) the scarps are fresh and cut present-day topography (Figures 2b and 3), and (2) the streams have been unable to erode away the ridges that dam the sagponds. A clear example of the latter is exposed in Cerro Tocoasi, 2 km SSW of Cabana Conde (Figure 2a), where two small sagponds are preserved in a gully, sloping at about 20°, carved in the crest of the hill.

Other arguments may be drawn from the space-time relations of the faults with the geological units that they cut. The most recent units are the somewhat indurated slope deposits of periglacial origin faulted along the right bank of Quebrada Trigal (Figure 3, see detailed study in the next section). These rather stratified, angular, slope deposits (c, Figure 3) bury older soils (d, Figure 3) and are covered only by the thin present-day soil (a, Figure 3). We relate these slope deposits (c) with the last cold epoch which is commonly considered to be grossly coeval with the Wisconsinian glacial epoch (roughly 10,000 to 50,000 years B.P.) of North America (Clapperton, 1972; Mercer and Palacios, 1977; Servant, 1977). The youngest faulted andesitic flows (Mucurca flows V3, Figure 2a) originated from a vent located 2 km north of lake Mucurca and flowed northward across the main lava plateau. They damed lake Mucurca and filled its wide outlet valley. This small vent (altitude 4550 m) and part of the flows rest upon the distal moraines that cover the western slope of the huge eroded Lipayoc caldera. These moraines are unconsolidated, have a fresh morphology, and crop out down to an altitude of 4400 m. These criteria are shared by many moraines related to the last Andean glacial epoch in southern Peru. The Mucurca lava flow is thus probably younger than the "Wisconsinian epoch." Some vents are located directly along the faults: the Uncapampa volcanic vent, located 7 km north of Huambo, lies over a N82°E trending fault that appears to be the western prolongation of the Solarpampa fault. The neck (altitude 4210 m) standing 7 km to the N22°E of Huambo is also located on the Solarpampa fault.

A closer examination of the relations between the faults and the lava flows both at the Uncapampa vent and where the Solarpampa fault crosses the Mucurca (V3) flow shows that faults have been reactivated several times. Therefore their

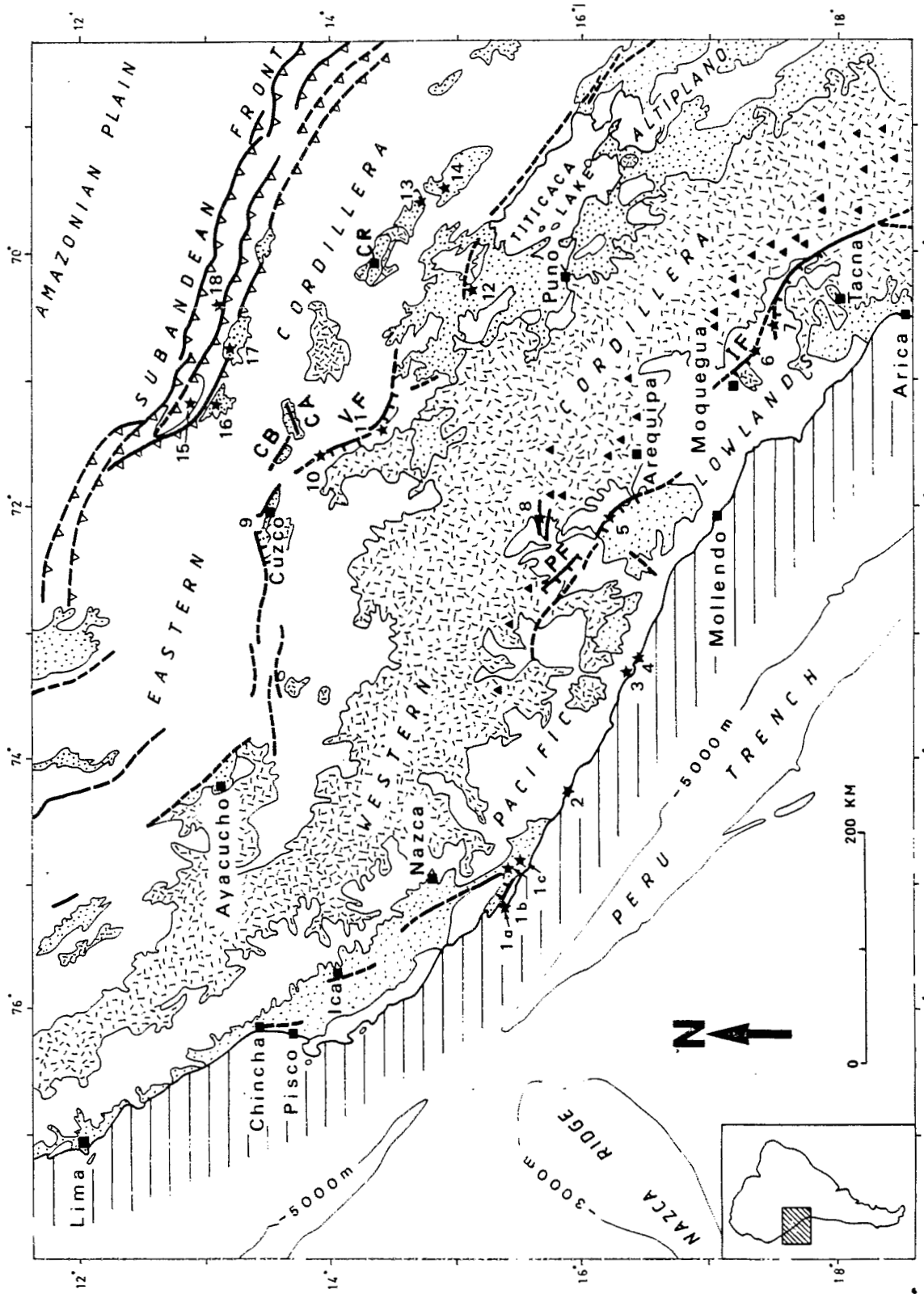
AMAZONIAN PLAIN
SUBANDEAN FRONT
EASTERN CORDILLERA
WESTERN CORDILLERA
ALTIPLANO
LOWLANDS
PACIFIC
PERU -5000m TRENCH
NAZCA RIDGE -3000m
TITICACA LAKE
CB
CA
VF
CR
PF
IF
Cuzco
Puno
Arequipa
Moquegua
Tacna
Arica
Mollendo
Nazca
Ica
Pisco
Chincha
Ayacucho
Lima
-5000m
200 KM
0
N

Fig. 1. Locations of Quaternary fault sites analyzed in this paper. Numbers are the same as in the text and in the other figures. Thick solid lines are major Quaternary faults observed in the field (hatchured on the downthrows). Thick dashed lines are inferred Quaternary faults. Thick lines with attached open triangles are major Subandean reverse faults. Major fault zones with Quaternary normal displacements: CA, Cordillera del Ausangate faults; CB, Ccatca basin fault; CR, Crucero basin; IF, Incapuquio fault; PF, Pampacolca fault; VF, Vilcanota fault. Solid triangles are Recent or active volcanoes; shaded areas are Neogene and Quaternary volcanics, stippled areas are Plio-Quaternary basins.

movements are in part contemporaneous with lava eruptions. The recent V3 Uncapampa volcanoe vented fluid basic andesites toward the west and NW (Figure 2a). The vent consists of two horseshoe-shaped inset sommas that are widely opened northwestward and are filled by a younger central flow. Two minor E-W faults cut both sommas but do not cut the central flow (Figure 2a). As the state of erosion, weathering, and morphology of all the flows vented from Uncapampa crater is the same, it can be assumed that they are related to an almost single venting episode in part coeval with tensional tectonics along the E-W trending normal faults. Analysis of the relations between the different flow units of the Mucurca flow and the Solarpampa fault also demonstrates that this fault moved at the time the lavas were flowing. In the older volcanics V2, the fault throw is larger than in the Mucurca V3 flow (Figure 2a). Upstream, i.e., south of the fault, the western part of the V3 flow has been ponded along the already existing scarp, built into V2 lavas, giving a peculiar arrangement of the large pahoehoe waves on the flow surface. Once the pond had been filled by the older part of V3 flow, the younger one was able to flow freely downstream and fill the valley farther north. A later normal movement along the same Solarpampa fault again depressed the southern block. These data indicate that the Solarpampa fault has moved at least twice during its Recent history. Similarly, the throw of the Trigal fault at the Pampa Trigal site (see next section) is greater than 10 m in the V2 volcanics and only about 4 m in the slope deposits (Figure 3).

Structural analysis of Trigal site. The volcanic nature of the material and the lack of good outcrops make a detailed kinematic analysis of the Huambo-Cabana Conde fault system difficult. Only in the Quebrada Trigal, a fresh roadcut along the new Huambo-Cabana Conde road allowed us to study in some detail the striations of a faulted zone associated with the Trigal fault (Trigal site, Figures 2a and 3). The throws of individual faults range between 1 dm and 1 m. The movements are very recent because these faults cut periglacial slope deposits (c, Figure 3) related to the last glacial epoch (see prior section). In addition, the present-day soil (a, Figure 3) appears to be slightly faulted. These slope deposits are

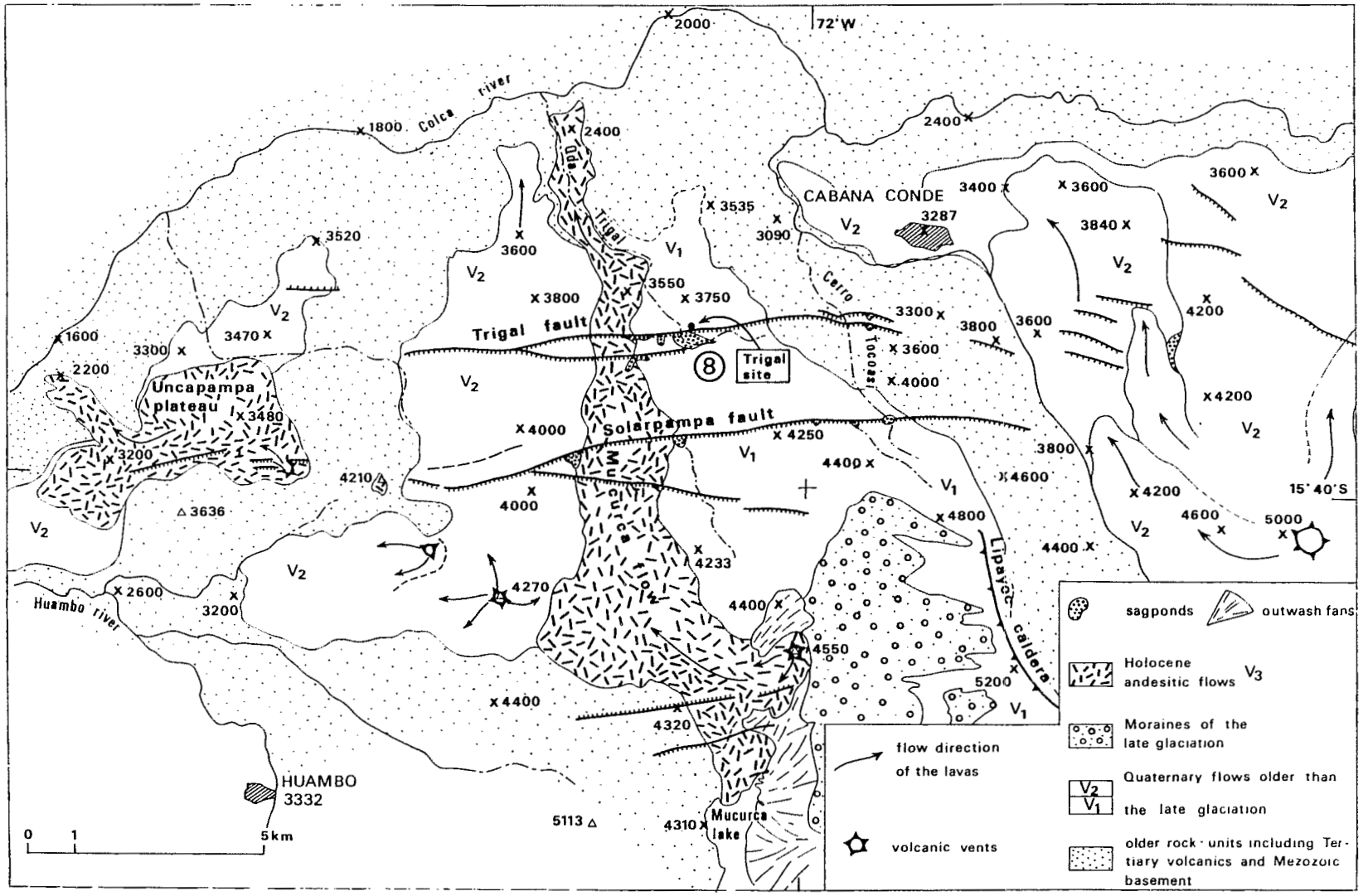

Fig. 2a. Geological map of the Huambo-Cabana Conde area (Western Cordillera), 100 km north of Arequipa (see location in Figure 1, point 8). The lava plateau, at a mean elevation of 4 km, is crossed by the major normal Trigal and Solarpampa faults (thick lines hatchured on the side of the downthrown block). The faults offset the andesitic Mucurca flow of post late glacial epoch. Kinematics of the Trigal fault analyzed in detail at Trigal site (point 8) indicate a nearly N-S trending extension (Figure 4, site 8).

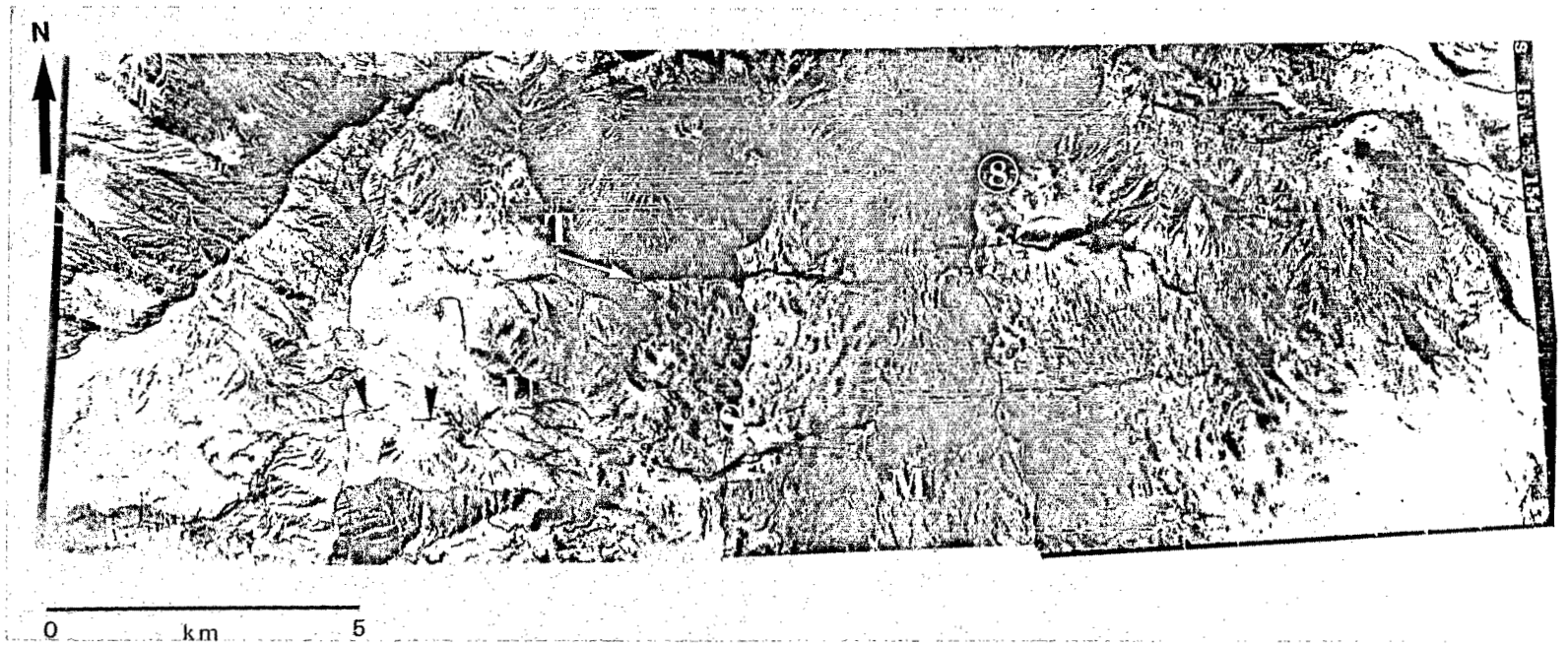

Fig. 2b. Aerial photograph covering the central part of the Huambo-Cabana Conde area seen on Figure 2a. Most of the andesitic flows are directed northward as the Mucurca flow (M). The Trigal (T) and Solarpampa (S) normal faults are the most prominent structures seen on the aerial photograph. The minor Uncapampa vent (U) and the minor E-W trending faults (small arrow heads) cut flows produced by this vent. The Trigal site (Figure 3) is shown by a small arrow marked tr.

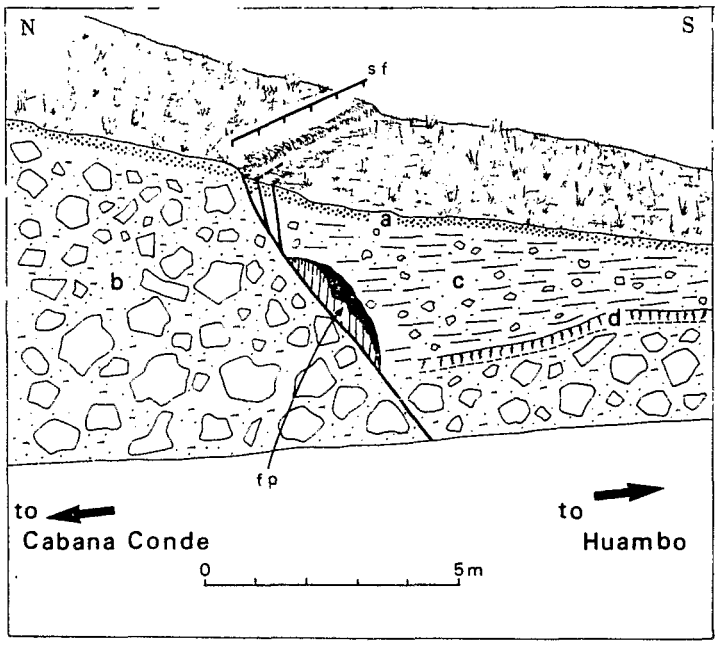

Fig. 3. Field view of the Trigal fault at Trigal site (Figures 2a and 2b, point 8) along the Huambo-Cabana Conde road. Symbols are as follows: a, present-day soil; b, slope breccia made of volcanic deposits being a lateral equivalent of the Vl lava flows; c, slope deposits related to the last glacial epoch; d, paleosoil between b and c units; sf, fault scarp; fp, fault plane. Striations have been measured on fault planes within the same Trigal fault zone (Figure 4, site 8).

somewhat consolidated because they have a well-developed sandy-clayed matrix which contains only few scattered rock fragments. At the scale of the outcrop, material has an homogeneous behavior. Moreover there is no evidence of fault plane rotation, as the original bedding does not appear to be warped.

Twelve striated normal slickensides were measured. It clearly appears that the kinematics of these faults (Figure 4, site 8) agree better with a roughly N-S lengthening. To define more accurately the directions of Recent and active extension, we model brittle deformation considering the fact that the rocks are highly fractured and blocks are rigid. It is current practice to model deformation of highly fractured bodies of rocks which have been subjected to a stress field by using a simple mechanical system (Carey and Brunier, 1974; Carey, 1976, 1979)(see the appendix). This supposes that the bulk change of the geometry of the rock body occurs through the addition of independent and small displacements of rigid blocks. If the slips on the faults are independent, then the slip S given by the striations on each fault plane has to be parallel to the tangential stress t resolved on each fault plane. Inversion of data yields the azimuth of the principal stress axes and a ratio R of the principal stress differences such as $R=(\sigma 2-\sigma 1)/(\sigma 3-\sigma 1)$.

For the Trigal site (Figure 4, site 8), although the striated slickensides are only 12, they are rather well spatially distributed and thus enable a computation. The obtained solution (site 8, Table 1) appears to be good because the angles (t,S) between the predicted t and the observed S striations are always less than 20° (see histogram, Figure 4, site 8). The minimum "tensional" principal stress (σ 3) direction has an azimuth of N10°E, the intermediate deviatoric principal stress value (σ 2) is "tensional" but of much smaller magnitude than the minimum principal stress, as shown by the ratio R=0.77. Therefore the Recent and probably active state of stress of this area implies a nearly N-S trending extension. At least part of the recent volcanic

activity of the Western Cordillera is associated with this N-S trending tensional tectonics.

This appears to have a regional meaning since it is in very good agreement with the occurence of E-W trending andesitic dykes at Achoma in the Chivay basin which is located 30 km farther east of Cabana Conde. Unpublished K-Ar dates (G. Feraud, written communication, 1984) from these Chivay volcanics and from the basal part of the Huambo-Cabana Conde recent volcanics (V2 in Figure 2a) confirm the Pleistocene age of these rocks (ages between 0.2 and 1 m.y. B.P.) and therefore of the N-S extensional tectonics.

Quaternary and Active Normal Faults along the Northeastern Altiplano

Around Lake Titicaca, Quaternary lacustrine terraces and coeval erosional surfaces are well preserved. They do not show clear offsets due to normal faulting except along the northeastern border of the Altiplano (Lavenu, 1981; Sébrier et al., 1982; Lavenu et al., 1984). There, Quaternary normal faults have been described, and their kinematics are in agreement with roughly N-S striking extension (Lavenu, 1978; Bles et al., 1980).

From a general point of view, extensional deformation appears to be small on the Altiplano and along its southwestern margin. However, normal faulting is clear in its northeastern part and in the transitional zone with the Eastern Cordillera. Here we describe the normal faults that we observed on the Peruvian Altiplano and its northwestern continuation as far as the Cuzco basin (Figure 1).

The Cuzco basin faults. The Cuzco basin is a small intra-Andean basin located between the Eastern Cordillera and the High Plateaus (Figures 1 and 5a). It is partly infilled by Quaternary continental deposits (Sébrier et al., 1982; Cabrera, 1984). To the north, this basin is limited by the Tambomachay active fault which is about 20 km long (Figures 5a and 5b) and exhibits a 2-m-high south facing morphological scarplet (Figure 6). This fault has a nearly N90° to N120°E trend and a mean dip of 60° to the south. At its western end, a west facing scarplet appears; this N-S striking recent fault shows also a normal downthrow. Thus all the recent faults have a clear normal component (Figures 6 and 7, site 9). The approximately 300-m-high south facing scarp which dominates the 2 m high scarplet (Figure 6) indicates that the Tambomachay fault has moved several times during the Pleistocene, producing a cumulative normal throw that may attain 300 m.

Striated fault planes have been observed in several places (a, b, c, d, Figure 5a) in the vicinity of the major fault and near San Sebastian. On the major fault zone, two or three superimposed families of striations are clearly seen. The first one shows a reverse sinistral strike-slip motion which agrees with an E-W shortening and is responsible of the linear trace of the Tambomachay fault. The last one shows a normal strike-slip movement which agrees with a N-S lenthening (Figure 7, site 9). This is the last kinematics which has probably produced the normal scarp seen in the field (Figure 6). Near San Sebastian, faults have throws which range between several decimeters and 3 m. They are Pleistocene to very Recent in age because they offset Quaternary deposits and postdate compressional deformation which affects early Pleistocene lacustrine beds (Figure 5a).

It is easily seen (Figure 7, site 9) that normal faults having a NW-SE direction show a clear sinistral strike-slip component so that extension does not appear orthogonal to the Andean belt strike. Inversion of the data for the two sites gives minimum principal stress (σ 3) directions striking to the N186°E (Table 1, site 9d) and to the N18°E (Table 1, sites 9a, 9b, 9c). Grouping all the normal slickensides measured in the Cuzco basin (Figure 7, site 9), we obtain a solution of good quality (site 9, Table 1), 16 striations having an angle (t,S) lesser than 20° (see histogram 9, Figure 7). The stress field in the Cuzco basin is enough homogeneous to give a quite reliable result. The azimuth of the minimum principal stress is N8°E. Therefore the Recent state of stress in the Cuzco basin appears to be characterized by a nearly N-S trending extension as in the Western Cordillera (see above section) and on the northern Bolivian Altiplano.

The Vilcanota river fault system. The roughly E-W trending Cuzco fault zone is relayed to the SE by a NNW-SSE striking fault system which controls the direction of the Vilcanota river valley (VF on

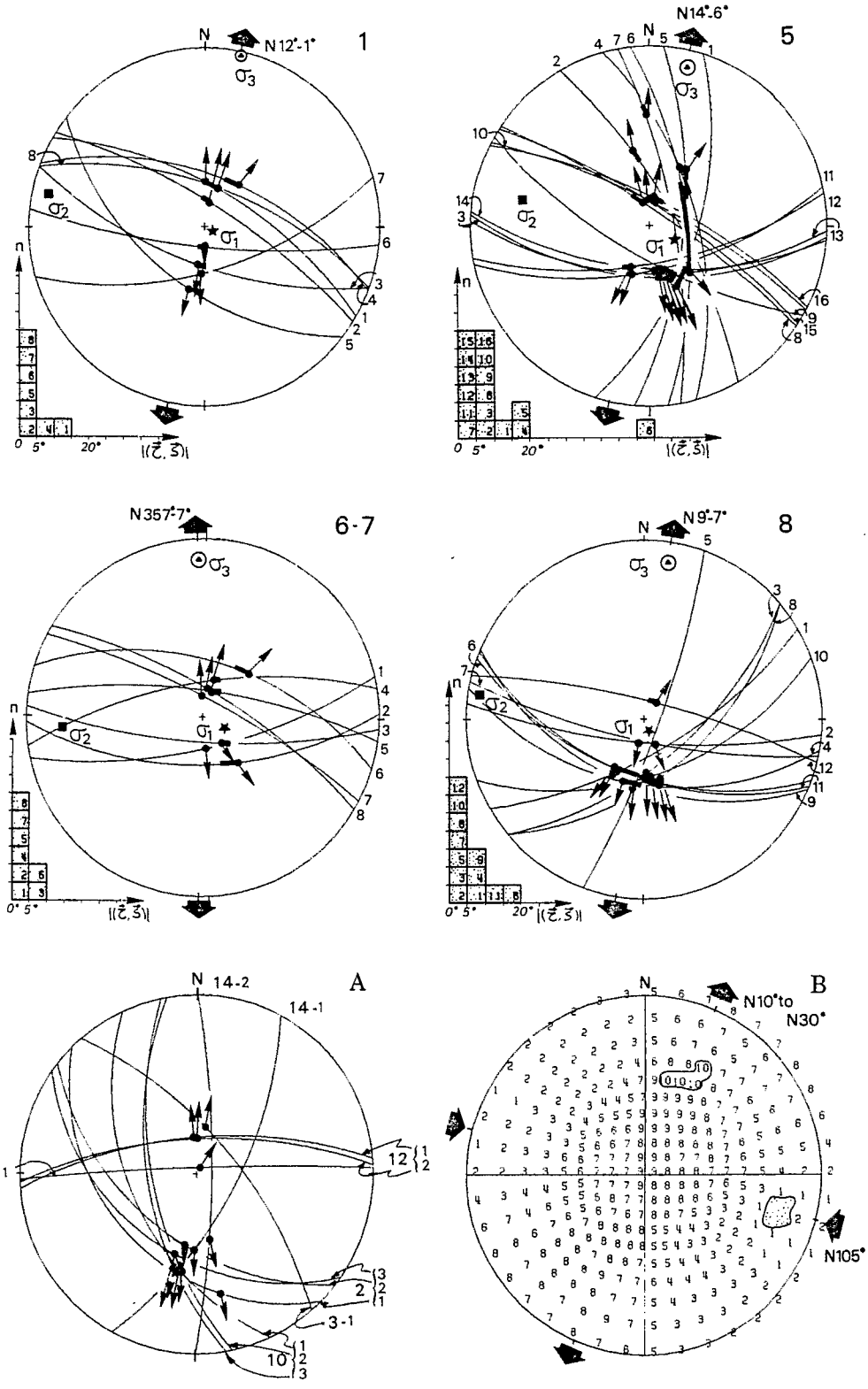
N12°-1°
1
N14°-6°
5
N357°-7°
6-7
N9°-7°
8
N 14-2
A
B
N10°to
N30°
N105°

Figure 1). Its length is about 90 km from Urcos to Langui Layo lake (Figure 8a) and its width varies between 10 and 20 km. The Vilcanota river fault system separates the Meso-Cenozoic High Plateau terranes to the SW from the Paleozoic formations of the Eastern Cordillera to the NE. It vanishes to the SE at the northwestern termination of the Altiplano basin. Fault movements have produced an uplift of the Eastern Cordillera with respect to the High Plateau. Shoshonitic Quaternary volcanoes (Lefevre, 1973) crop out along the Vilcanota valley.

Evidences of the most recent faulting are located mainly 5-10 km west of the Vilcanota valley along a 70-km-long lineament (Figure 8a). This is underlined by a series of lacustrine basins whose altitudes range between 3650 and 3950 m. The most important of them are the Pomacanchi lake to the NW and the Langui Layo lake to the SE (Figure 8b). Several times, small historical earthquakes (Silgado, 1978) have destroyed villages along this lineament (crosses on Figure 8b). Their foci were estimated to be very shallow. NW of the Pomacanchi lake, a 6-km-long fault trace is clearly seen in the field and on the aerial photographs (Suarez et al., 1984 Figures 15 and 14), and also on Landsat imagery (Figure 8b). This Pomacanchi fault has a N140°E strike and a 60°-70° dip to the SW; it exibits a 50-m normal throw of Quaternary age. It cuts alluvial conglomeratic fans related to the penultimate glacial epoch (not accurately dated but more than 0.1 m.y.). However, where streams cross the fault, the two last alluvial terraces do not show any evidences of offset. Taking into account the accepted chronology of alluvial formations in south Peru (Sébrier et al., 1982), the last fault movement is Recent, roughly between the last and the penultimate glacial epochs, but does not appear active (i.e., last movement older than 10,000 years B.P.). However, some parts of the Vilcanota river fault system must be active as shown by the historical seismicity and fresh scarplet affecting the present-day morphology north of the Langui village (star 11, Figure 8a).

Three striated fault planes have been measured on the southeastern part of the Pomacanchi fault (Figure 1, point 10). They show a normal sinistral strike-slip movement (data 10: 1, 2, 3, Figure 4, A). These limited data do not permit computation of the extensional direction. However, as other spread fault data of southern Peru, they are in agreement with a N-S trending extension (Figure 4, A).

The Mataro faults. Ten kilometers WNW of the northwestern termination of the Titicaca lake (Lago de Arapa), at an elevation of 3950 m (Figure 1, point 12), the lacustrine Mataro formation represents deposits of the lower Pleistocene Titicaca lake (Lavenu et al., 1984). Two small

---

Fig. 4. (opposite) Normal fault data from Pacific Lowlands and Western Cordillera used to compute solutions of Table 1 (locations on Figure 1). Numbers outside stereonets refer to data inside the histograms. Arrows attached to fault traces correspond to the measured slip vectors S (Wulff stereonet, lower hemisphere). Thick segments on fault traces and histograms show deviations between measured S and predicted t slip vector for each fault plane. Large black arrows give azimuths of the minimum σ 3 computed principal stress directions. Note that they strike nearly N-S for all the analyzed sites. (A) Normal fault spread data from Pacific Lowlands and from High Andes. Large numbers outside the stereonet refer to location of the sites (Figure 1), and small numbers refer to fault data. Fault kinematics are in good agreement with roughly N-S trending lengthening. (B) Compressional and extensional directions deduced from focal mechanisms of 11 earthquakes located under the transitional zone between Pacific Lowlands and High Andes (data obtained from a local seismic network, depth foci between 12 and 40 km Grange, 1983). Extensional and compressional quadrants are superimposed and thus define common extensional and compressional zones. A counting grid is built on the lower hemisphere with points as centers of circles whose surfaces are 1% of the hemispere surface. Numbers on stereonet B represent the number of times such a defined small circle is common to the extensional zone defined as above (density diagram, Wulff stereonet, lower hemisphere). Ten focal mechanisms define two small areas (number 10 and shaded areas) which respectively contain the common extensional direction (divergent black arrows) and the common compressional direction striking roughly N105°E (convergent black arrows). One focal mechanism (Grange's event 836) is not in agreement with the other 10 solutions.

TABLE 1. Parameters of the Deviatoric Stress Tensors Computed From the Quaternary and Recent Normal Faults of the High Andes and Pacific Lowlands

Site	ND	Latitude S	Longitude W	Principal Stress Directions σ 1 Azimuth	σ 1 Dip	σ 2 Azimuth	σ 2 Dip	σ 3 Azimuth	σ 3 Dip	R
1	8°	15°22'	75°09'	115°	84°	282°	06°	012°	01°	0.79
5	16°	16°11'	72°02'	121°	71°	282°	18°	014°	06°	0.71
6-7	8°	17°28'	70°28'	115°	75°	266°	13°	357°	07°	0.83
8	12°	15°38'	72°01'	161°	82°	279°	04°	009°	07°	0.77
9	19°	13°30'	71°56'	324°	80°	097°	07°	188°	07°	0.42
9a-b-c	13°	13°30'	71°56'	184°	82°	287°	02°	018°	08°	0.59
9d	6°	13°30'	71°56'	321°	74°	094°	11°	186°	11°	0.39
13	18°	14°41'	69°30'	121°	81°	265°	07°	356°	05°	0.79
13b	6°	14°41'	69°30'	170°	80°	267°	01°	356°	10°	0.77
13c	9°	14°41'	69°30'	099°	80°	267°	10°	357°	02°	0.76

These parameters are computed from superficial Quaternary and Recent normal faults of Pacific Lowlands (sites 1, 5, and 6-7) and of High Andes (sites 8, 9, 9a-b-c, 9d, 13, 13b, and 13c). Site localizations are shown on Figure 1. ND is the number of triated fault planes used to compute the solutions. Azimuths are measured clockwise from north; dip is toward the measured azimuth. $R = \sigma'2-\sigma'1/\sigma'3-\sigma'1$ is the "stress ratio" or "shape factor" of the stress tensor. Its value varies between two extremes: 0 as $\sigma'2 = \sigma'1$ and 1 as $\sigma'2 = \sigma'3$. Computed normal faults are on stereonets of Figures 4 and 7.

faults have been observed on a 10-m-high flank of an intermittent stream, cut into the Mataro formation. They have an E-W strike and a 70° dip to the north with a 10- to 20-cm normal throw. They are antithetic faults with respect to major faults bordering the lake Titicaca to the NE. Although they are small, these faults may be indicative of the Quaternary deformation on the Altiplano because they are situated between the Vilcanota river fault system and the Bolivian Altiplano Quaternary faults described by Lavenu (1978). Moreover, their kinematics (data 12: 1, 2, Figure 4, A) are also in agreement with a N-S striking lenthening.

Quaternary Normal Faulting in the High Basins of the Eastern Cordillera

North of Lake Titicaca, several Quaternary intermontane basins are situated within the central part of the Eastern Cordillera at an elevation of 4000-5000 m (Figure 1, points 13, 14, and CA, CB, CR). Evidence of Quaternary normal faulting have been observed mainly in the Ananea basin (Figure 1, point 13) but also in the Peruvian part of the Ulla Ulla basin (Figure 1, point 14).

The Ananea basin faults. The WNW-ESE trending Ananea basin has a mean elevation of 4600 m (Figure 1, point 13). As for the Altiplano, its general structure results mainly from Neogene compressional deformations. The Plio-Pleistocene Ananea depression is superimposed on the ESE termination of a broad synclinorium in the center of which Oligo-Miocene formations crop out; this synclinorium extends to the NW as far as the Crucero basin. This Ananea basin (Figure 9) is infilled by Pliocene palustrine sediments and by several Pleistocene moraines and outwash deposits (Fornari et al., 1982).

In this basin, we measured Quaternary normal faults at three different points (13a, 13b, 13c on Figure 9): three at Viscachani (13a), six at Rinconada (13b), and nine at Pampa Blanca (13c). Each of these three points is less than 5 km distant from each other. Normal faults have been observed along distances that range between several decameters to several hectometers. Their throws vary from several decimeters up to 6 m. These normal faults postdate compressional tectonics which deformed Pliocene and early Quaternary deposits. Moreover, some of them offset moraines which are related to the penultimate glacial epoch (older than 100,000 years B.P.). The age of the normal faulting is thus Quaternary. Faults having an E-W direction are nearly purely

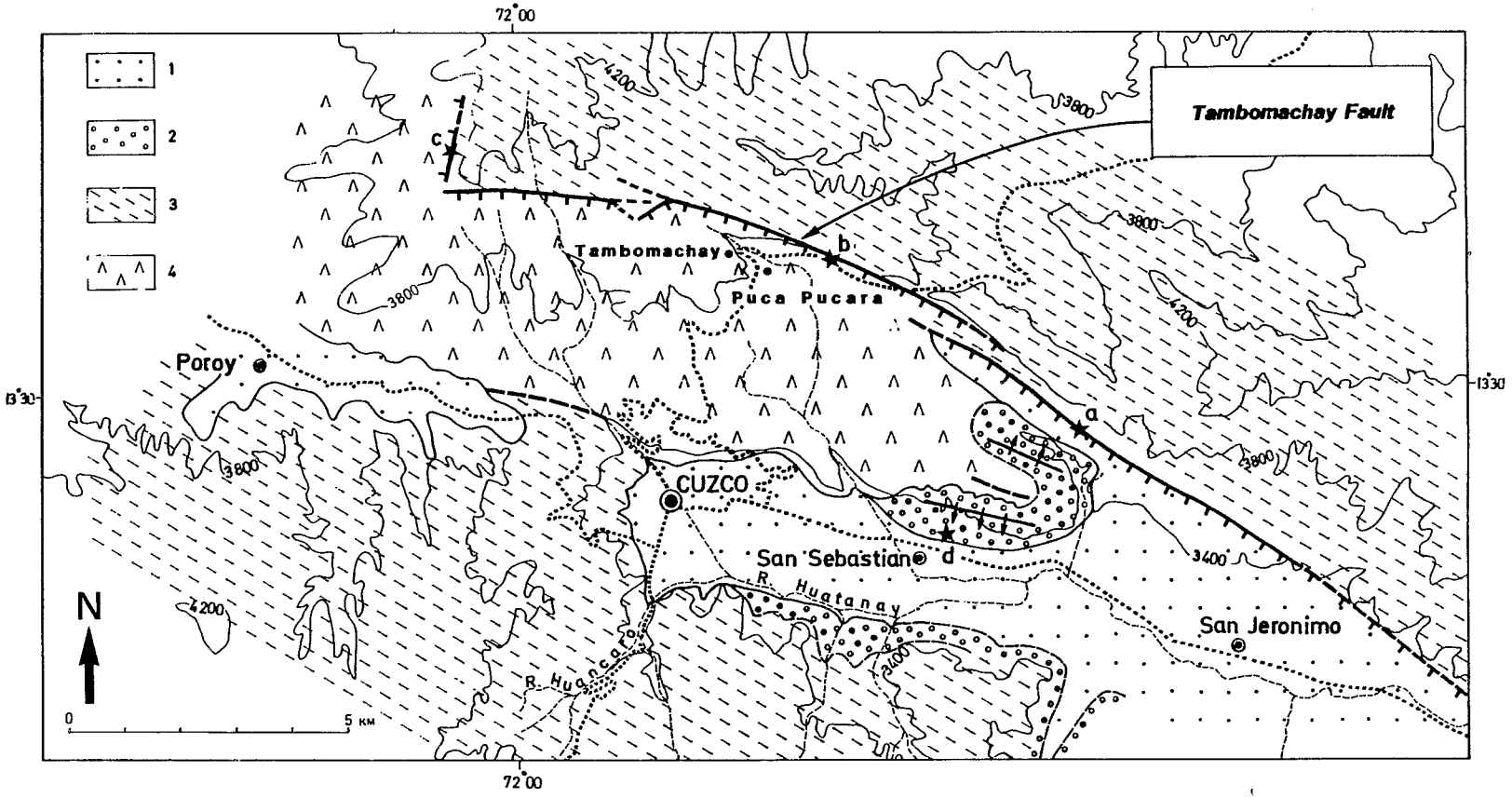

Fig. 5a. Structural sketch of Cuzco basin faults (Figure 1, point 9). 1, Recent Quaternary formations; 2, early Pleistocene San Sebastian formation; 3, Paleogene red beds; 4, Cretaceous Yuncaypata formation. Roads: dotted lines. Tambomachay active normal fault: thick lines (downthrown block hatchured). Fault kinematics analyzed in the vicinity of the fault (stars a, b, c; sites 9a-9c, Figure 7) and near San Sebastian (star d; site 9d, Figure 7) show normal slip with a small sinistral component on the major fault. North of San Sebastian, early Pleistocene lacustrine beds form kilometric monoclines (arrows strike toward the higher dip) which result from compressional deformation not present in Recent Quaternary deposits.

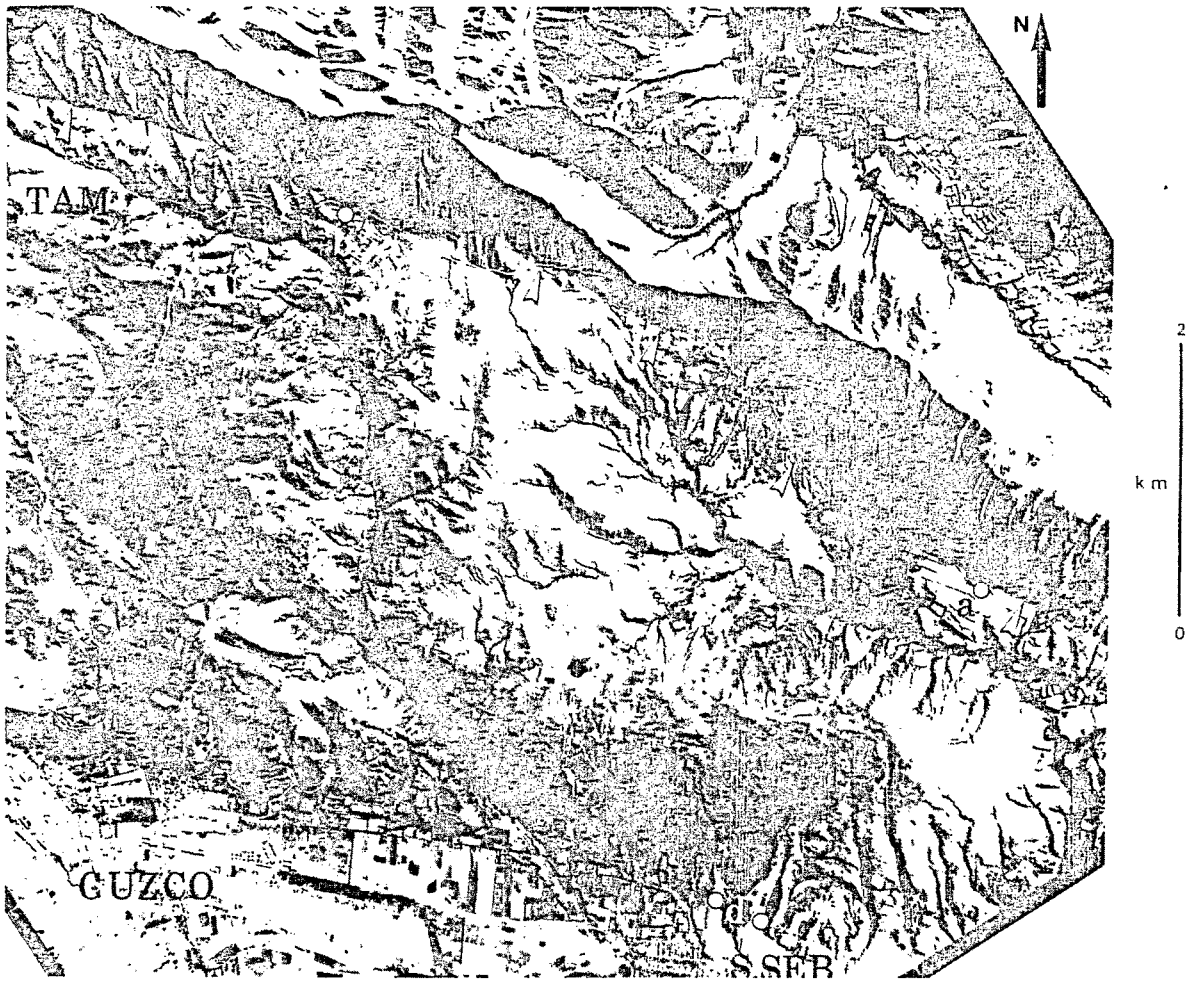

Fig. 5b. Aerial photograph covering central part of Cuzco basin (see Figure 5a). Most prominent structures are the two segments of the Tambomachay active fault (small black arrow heads). Analyzed fault sites are marked by solid circles a, b, d as on Figure 5a. TAM, Tambomachay; PU, Puca Pucara Incaic archeological sites; S. SEB, Cuzco suburb of San Sebastian. NNE of San Sebastian, early Pleistocene formation appears as a broad nearly symetric anticline.

normal; faults having a NE-SW direction are normal with a dextral strike-slip component, while faults striking NW-SE are normal with a sinistral component (Figure 7, site 13). These kinematics agree with a roughly N-S lengthening. Computation of the principal stress directions confirms this first inference.

We first processed separately the data from Rinconada (13b) and Pampa Blanca (13c) sites (Figure 7). The numerical results are good and comparable; they, respectively, show N4°W and N3°W trending extensional principal stress directions (13b and 13c, Table 1). Both computations used few data, and thus results are rather poorly constrained. We processed altogether the 18 data measured at the three studied points. This second computation has been possible because all the data had been collected in a small area and displacements are comparable in magnitude. The obtained solution (13, Table 1) yields a N4°W trending extension. This solution is of good quality, the (t,s) angles being lesser than 15° for all

Fig. 6. Field view of the Tambomachay fault seen toward the north from Puca Pucara (location: Figures 5a and 5b). A huge, south facing scarp (arrows) dominates the 2-m-high scarplet (small arrow heads). This indicates that the Tambomachay fault has moved several times during Pleistocene, producing a cumulative normal throw which is about 300 m.

the faults (see histogram 13, Figure 7). It is similar to the 13a and 13c solutions (see Table 1). Thus in the Ananea basin the Quaternary extension appears to have a nearly N-S direction.

The Tuncuchi faults. The Ulla Ulla basin, situated at a 4500-m elevation, has a flat topography. However, near Cerro Tuncuchi (Figure 1, point 14) a meander of the Suches river permits a good observation of two faults on a 25-m-high natural section. These faults have a N-S and N28°E strike, a steep dip to the east, and 0.5-1 m normal throws. They affect a sandy conglomeratic alluvial terrace of early Quaternary age and are covered by a distal outwash terrace which is not offset. Striations show normal dextral strike-slip movements (data 14: 1, 2, Figure 4, A). Although these faults are seen on a small exposure, they seems to be indicative of the Quaternary normal extension in the central part of the Eastern Cordillera since they are in good agreement with a N-S lenthening demonstrated in the nearby Ananea basin.

Other examples of Quaternary normal faulting in the Eastern Cordillera may include the N70°E trending faults that cut moraine deposits located to the north of the Cordillera del Ausangate (Audebaud, 1973) and the NE edge of the N125°E trending Ccatca basin (CA and CB on Figure 1). Unfortunately, we have not been able to carry out field studies on these faults.

COMPRESSIONAL TECTONICS IN THE SUBANDES

From the snow-capped summits of the northeastern edge of the High Andes, toward the Amazonian foothills the altitude decreases markedly; more than 3 km of vertical variation is observed along a 40-km distance. The stunted vegetation of the dry High Andes is replaced by the dense tropical jungle of the rainy sub-Andes. Field conditions become thus very difficult, and useful outcrops exist only along the torrential river banks (Figure

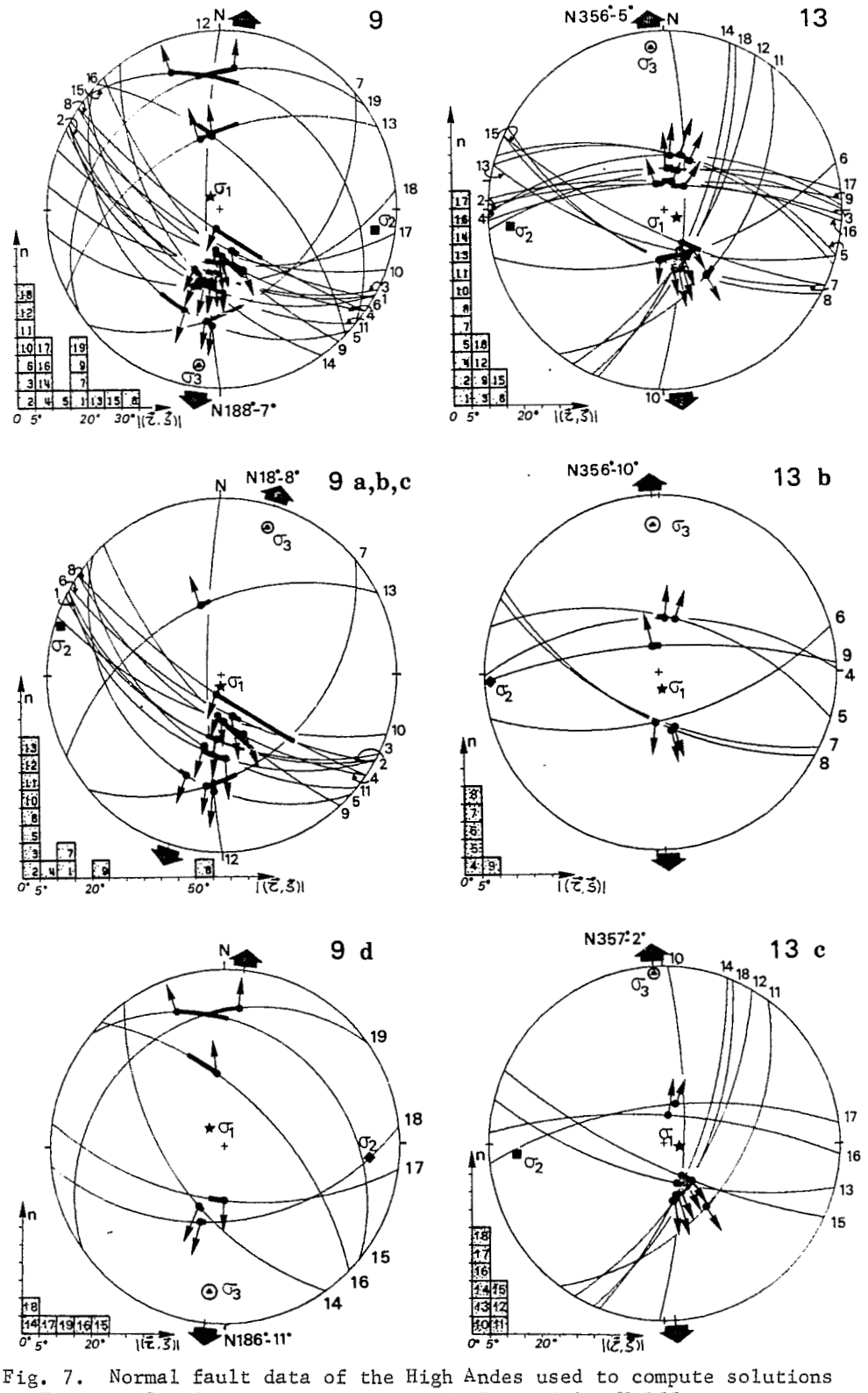

Fig. 7. Normal fault data of the High Andes used to compute solutions of Table 1. See locations on Figures 1, 5a, and 9. Wulff stereonet, lower hemisphere. Symbols as on Figure 4.

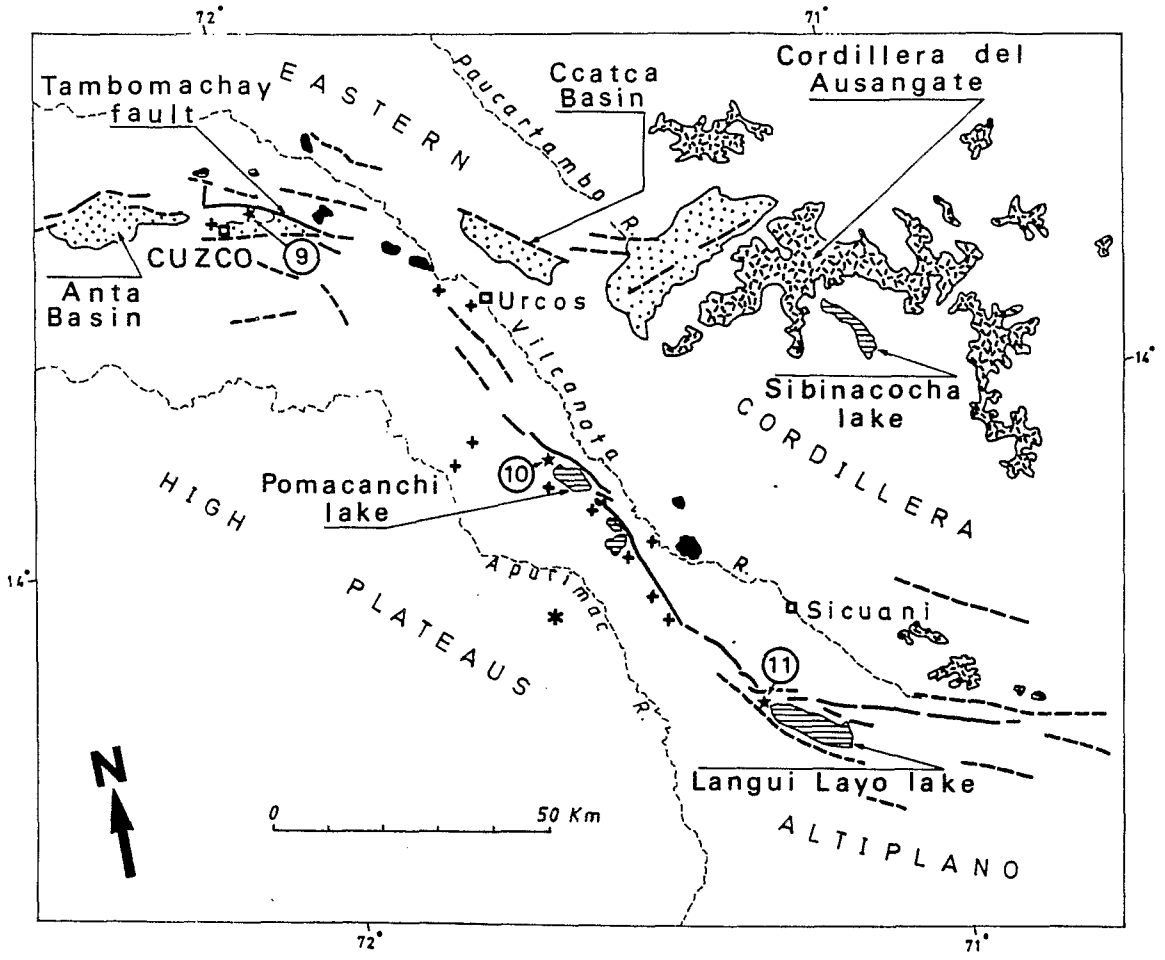

Fig. 8a. Structural sketch of the Vilcanota river fault system (High Andes, location on figure 1, VF and points 10 and 11). The roughly E-W trending Anta basin and Cuzco basin fault system is relayed to the SE by the NNW-SSE striking Vilcanota river fault system. This fault system disappears to the SE at the northwestern termination of the Altiplano. Thick solid lines are mapped normal faults; dashed lines are inferred Quaternary faults seen on Landsat images. Crosses, villages destroyed by small historical earthquakes; shaded areas, snow-capped summits of the Eastern Cordillera; stippled areas, Plio-Quaternary basins; solid patches, shoshonitic Quaternary volcanoes; asterisk, Quaternary volcanic cone. Orientation of the sketch is conform to the Landsat image orientation of Figure 8b.

10). Geological change is also conspicuous, the Eastern Cordillera consists mainly of Precambrian to lower Paleozoic metamorphic and intrusive rocks, whereas the sub-Andes are made of Cenozoic continental deposits (Figure 11).

The sub-Andean zone of south Peru is 500 km long and about 50 km wide (Figure 1). It corresponds to the northwestern part of the N120°E trending segment of the sub-Andes which extends for 1200 km from the lower Urubamba river (11° 30'S) to the Santa Cruz "elbow" (18°S). This narrow belt has an altitude which ranges between 300 and 1000 m and can be subdivided in two parts (Figure 11): (1) The Eastern Cordillera Piedmont basins (Pillcopata, Quince Mil, Candamo) form a string of Neogene-Quaternary alluvial fan basins located on a fault zone limiting the sub-

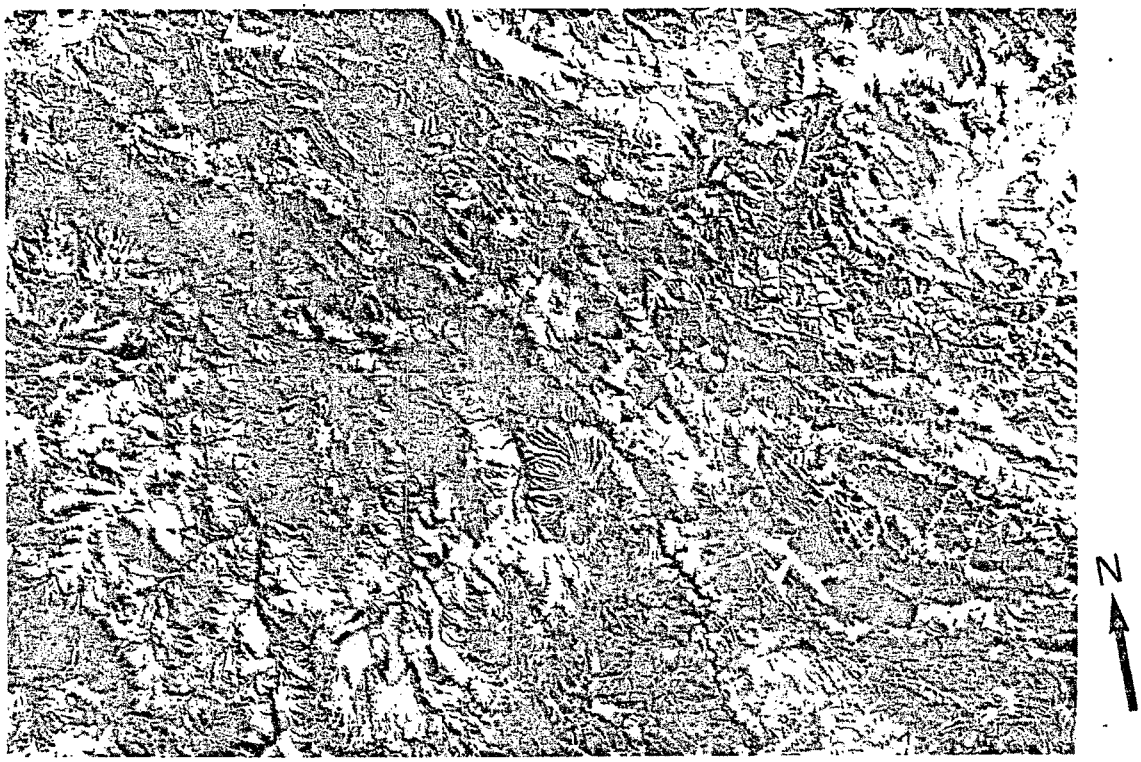

Fig. 8b. Landsat image MSS 7 (N. 8-2225- 14074-701) covering most of the structural sketch of the Vilcanota river fault system (Figure 8a). Snow-capped summits and Pomacanchi and Langui Layo lakes are readily compared with the structural sketch. Cuzco basin faults, Vilcanota river fault system, and Altiplano northern border fault system are marked by small arrow heads. Scale is given on Figure 8a.

Andes from the Eastern Cordillera. This fault zone is located at the foot of the High Andes, between 600 and 1000 m altitude. Deformation is characterized by reverse faulting and thrusting. (2) The sub-Andean hills (Salvacion, Mazuko), a 30- to 40-km-wide zone, are formed by ridges and vales, the altitudes of which are between 300 and 800 m. Deformation is characterized by folds and thrust faults affecting Neogene to early Quaternary sands and conglomerates. To the north, the sub-Andean zone is bounded by the Madre de Dios wide alluvial plain which appears to be the present-day aggradational piedmont. This limit between the sub-Andean hills, where erosion presently predominates, and the aggradational river plain should mark the active sub-Andean tectonic front.

Owing to unfavorable field conditions, only four areas (Quince Mil, Mazuko, Pillcopata, and Salvacion) have been analyzed. Taking advantage of two roads, we have reached the southern Peru sub-Andes, and then we have worked along the torrential river banks (Figure 10).

Eastern Cordillera Piedmont basins: Quince Mil and Pillcopata

The Quince Mil basin is situated at altitudes ranging between 500 and 900 m, is 40 km long and 15 km wide, and is infilled by coalescing alluvial fans that lie unconformably upon folded beds whose ages are upper Paleozoic, Cretaceous, and Paleogene. These alluvial fans include two series: (1) an older one attributed to Pliocene-early Quaternary, and (2) a younger one attributed to Pleistocene and Holocene (Laubacher et al., 1982). The older series consists of some 10-m gray carbonaceous sands preserved in channels and discordantly covered by about 250-m torrential conglomerates that are fairly consolidated and weathered. The younger series consists of unconsolidated alluvial fans and fluvial terraces. Series 1 has

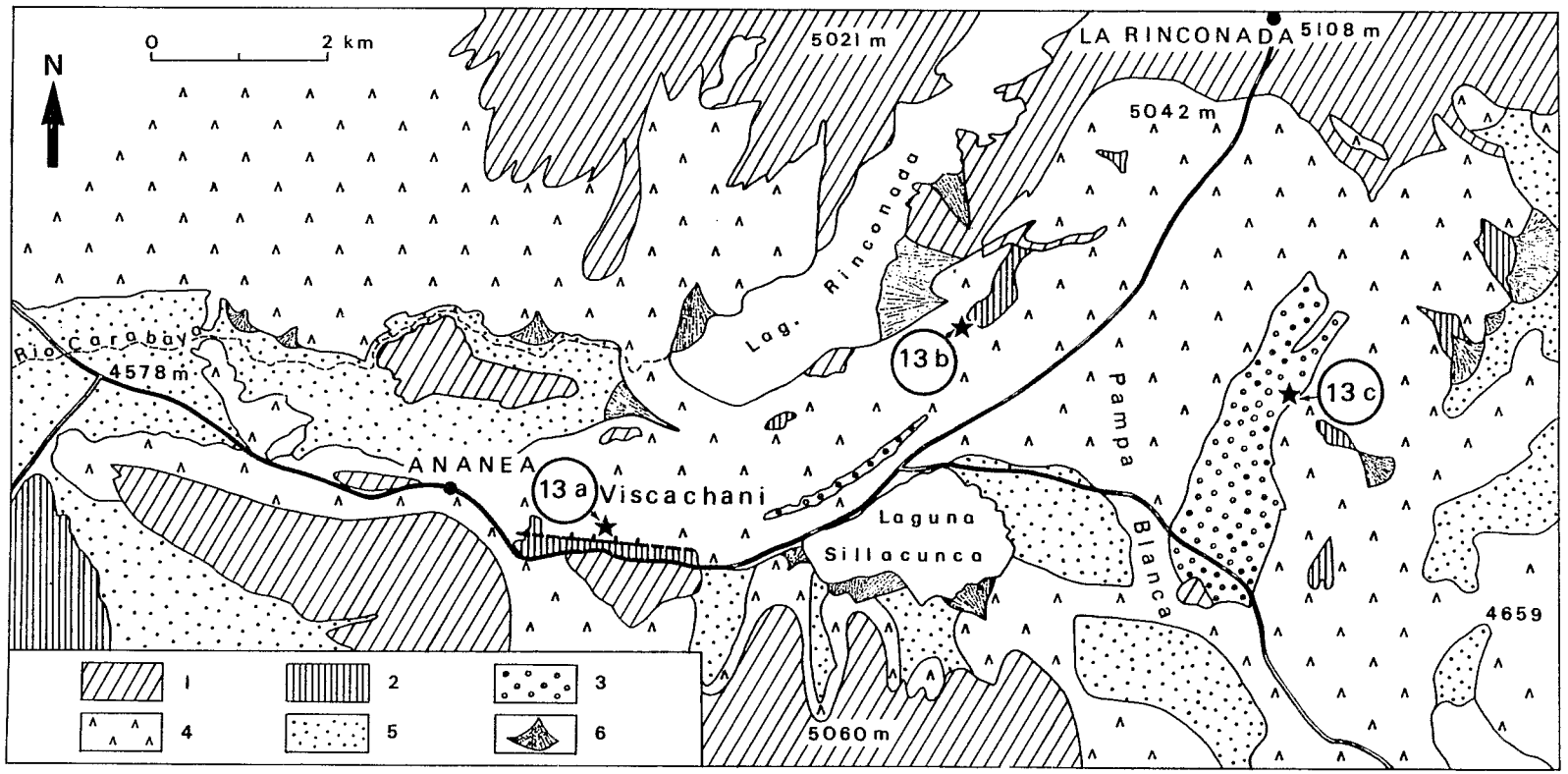

Fig. 9. Geological sketch of the eastern part of the Ananea basin (Eastern Cordillera, point 13, Figure 1). 1, Paleozoic formations; 2, Pliocene Arcoaja formation; 3, early Quaternary moraines and outwash deposits; 4, Recent and upper Quaternary moraines; 5, Recent outwash deposits; 6, Recent alluvial fans. Quaternary normal faults have been observed at three different places: at Viscachani (star a), at Rinconada (star b), and at Pampa Blanca (star c).

Fig. 10. E-W striking, south dipping reverse fault along the Palcamayo river, Quince Mil basin (site 17a, Figure 11). Fault (thick arrows) affects conglomerates of the Cancao formation, probably of early Quaternary age. Fault kinematics are in agreement with a N-S shortening (17a, Figure 12).

been deformed by reverse faulting, whereas no deformations have been observed in series 2. Thus the last deformations that we observed are not Recent and, as discussed below, are probably of early Quaternary age.

We measured reverse and strike-slip faults at two different points: along the Palcamayo river (Figure 12, site 17a) and along the Huajiumbre river (Figure 12, site 17b). These two points being 1.5 km distant. At the Palcamayo site, striations associated with reverse faults (Figure 10) were measured on flat sides of pebbles. Owing to the bad quality of Amazonian forest outcrops, generally it has not been possible to measure the throws of faults, but they can be estimated to be of the order of 1 m. At both sites, faults striking E-W have a nearly purely reverse slip, faults striking NE-SW have a sinistral reverse slip, and faults striking NW-SE have a dextral reverse slip (Figure 12, sites 17a and 17b). These kinematics agree with a roughly N-S shortening. Despite the poor quality of the data, computations of the principal stress directions (17a, 17b, Table 2) give good solutions (see histograms 17a, 17b, Figure 12) and confirm this inference. The maximum (compression) principal deviatoric stress directions strike to the N195° (site 17a) and N16° (site 17b). Therefore the last faulting observed in the Quince Mil basin is compressional and corresponds to a nearly NNE trending shortening.

These results are confirmed by observations made in the Pillcopata basin, which is located some 50 km to the WNW of the Quince Mil basin in a similar structural situation (Figure 11). It is situated at an altitude between 700 and 1100 m, and as the Quince Mil basin, it is infilled by coalescing alluvial fans. At Ubaldina, 2 km south of Pillcopata (Figure 11, site 16), in fluvial conglomerates similar to those of the older series 1 of the Quince Mil basin, we measured 12 striations associated with reverse faults (Figure 12, site 16). These striations postdate older ones which correspond to roughly E-W shortening (M. Sébrier et al., manuscript in preparation, 1985). As in the Quince Mil basin, the kinematics of the last faulting that we observed agree with a roughly N-S shortening. Although these data are not entirely in agreement with the hypotheses of the numerical model

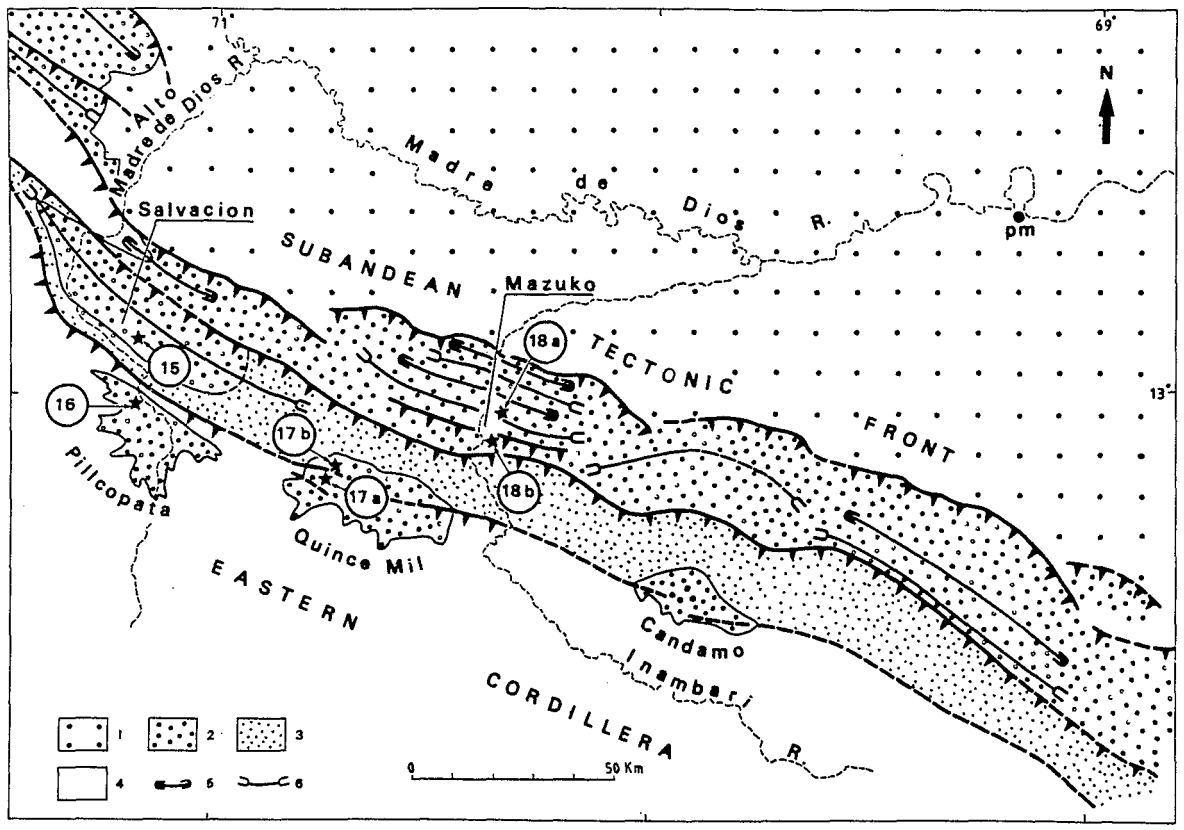

Fig. 11. Structural sketch showing situation of the studied Subandean segment of southern Peru (Figure 1, points 15, 16, 17, 18). Two structural situations are seen. The Eastern Cordillera Piedmont basins (Pillcopata, Quince Mil, Candamo) are located on a reverse fault zone (thick line) between 600 and 1000 m of altitude. The Subandean hills, between 300 and 800 m of altitude (Salvacion, Mazuko), are characterized by folding and high-angle thrusting (thick lines with attached solid triangles). 1, Recent Quaternary alluvial deposits; 2, Neogene and early Quaternary formations; 3, Paleogene red beds and upper Cretaceous sandstones; 4, Precambrian to lower Paleozoic metamorphic and intrusive rocks of the Eastern Cordillera; 5, anticline; 6, syncline. Numbered stars give situation of analyzed sites (Figure 12). All deformations are compressional, resulting from N-S trending shortening.

(see the appendix), the computed solution (16, Table 2) is fairly good (see histogram 16, Figure 12) and gives a N187° striking maximum principal stress (σ 1). Thus in two piedmont basins of the Eastern Cordillera the last deformations that we observed indicate a roughly N-S trending compression.

The Sub-Andean Hills: Mazuko and Salvacion

The Eastern Cordillera piedmont basins are separated from the sub-Andean hills by a small range of pre-Neogene rocks (Figure 11) that is either a faulted anticlinorium (i.e., Puente Inambari anticline between Quince Mil and Mazuko) or a complex faulted and folded zone (i.e., Pongo de Conec range between the Pillcopata basin and the Salvacion syncline).

The Mazuko area is located 20 km to the NE of the Quince Mil basin, along the lower Inambari river, at an altitude that ranges between 300 and 650 m (Figure 11). Upper Cretaceous to early Quaternary deposits are similar to those of the Quince Mil basin excepted that the Neogene to early Quaternary deposits (Mazuko formation) are thicker and do not rest unconformably on the Paleogene red beds. Thus there is no clear evidence for an

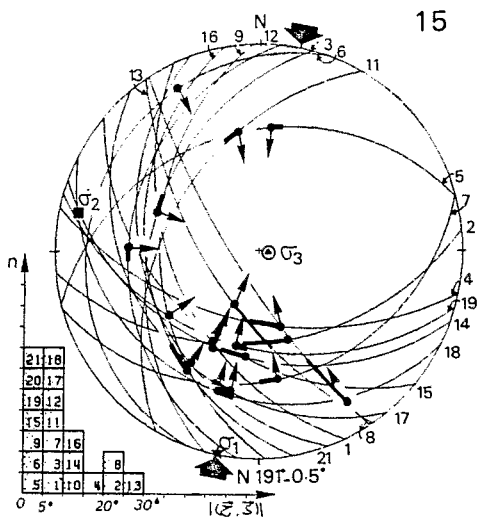
15
N
σ2
σ3
σ1
N 191°-0.5°
n
0 5° 20° 30°
|(z, s)|

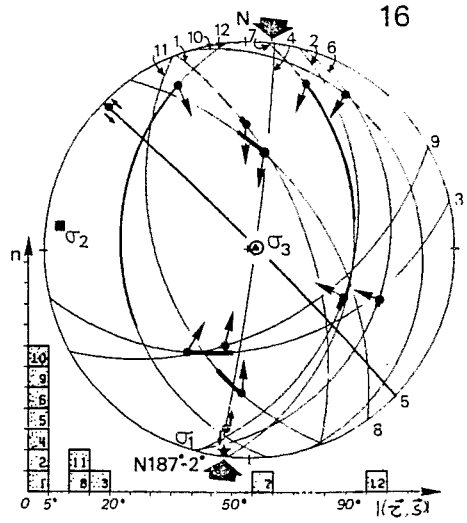
16
N
σ2
σ3
σ1
N187°-2°
n
0 5° 20° 50° 90°
|(z, s)|

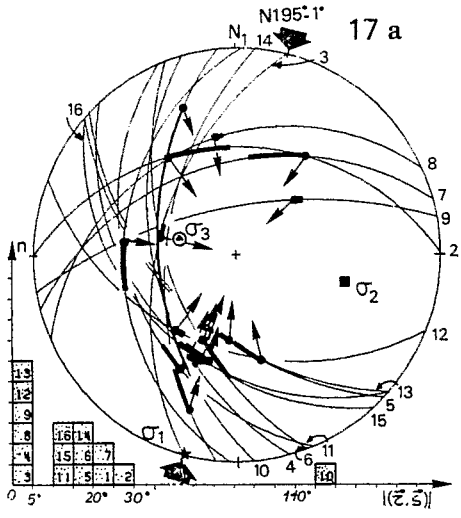
N195°-1°
17 a
N
σ3
σ2
σ1
n
0 5° 20° 30° 110°
|(z, s)|

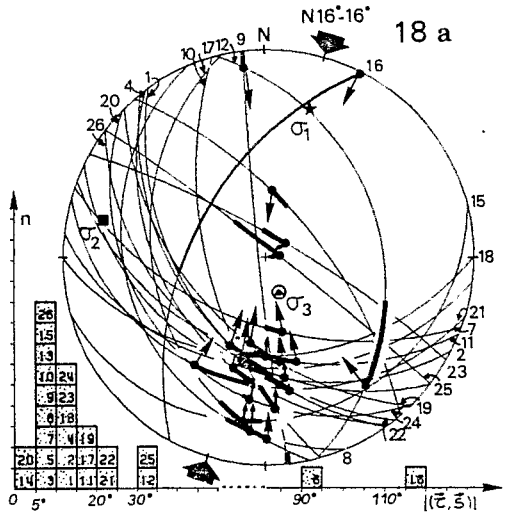
N16°-16°
18 a
N
σ1
σ2
σ3
n
0 5° 20° 30° 90° 110°
|(z, s)|

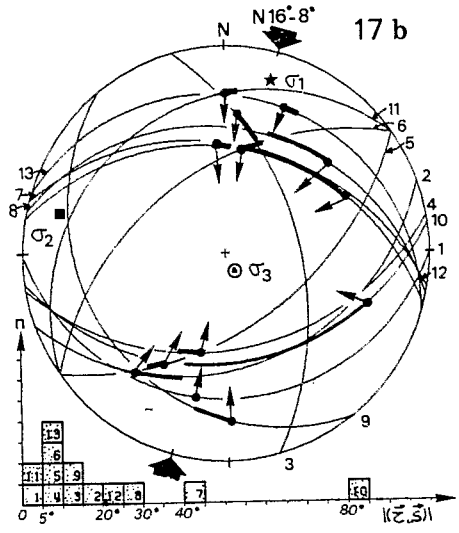
N16°-8°
17 b
N
σ1
σ2
σ3
n
0 5° 20° 30° 40° 80°
|(z, s)|

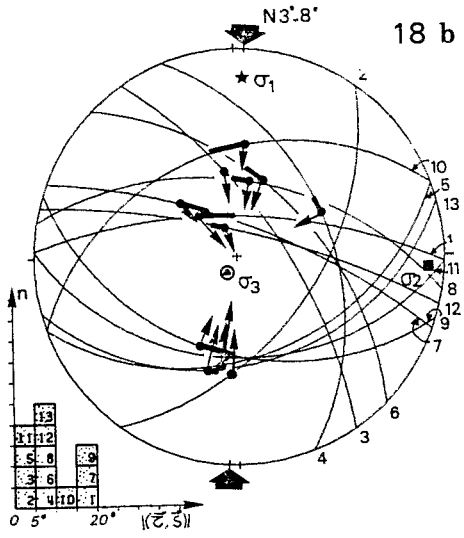
N3°-8°
18 b
σ1
σ2
σ3
n
0 5° 20°
|(z, s)|

TABLE 2. Parameters of the Deviatoric Stress Tensors Computed From Reverse Strike-Slip Vector Data of the South Peruvian Sub-Andes

Site	ND	Latitude S	Longitude W	Principal Stress Directions σ 1 Azimuth	σ 1 Dip	σ 2 Azimuth	σ 2 Dip	σ 3 Azimuth	σ 3 Dip	R
15	21	12°50'	71°20'	191°	0.5°	282°	05°	095°	85°	0.63
16	12	12°55'	71°23'	187°	02°	277°	04°	071°	86°	0.77
17a	16	13°12'	70°42'	195°	01°	105°	32°	287°	58°	0.63
17b	13	13°11'	70°42'	016°	08°	284°	10°	145°	77°	0.83
18a	26	13°05'	70°23'	016°	16°	283°	11°	160°	70°	0.54
18b	13	13°08'	70°23'	003°	08°	094°	05°	215°	80°	0.57

These parameters are computed from the reverse strike-slip vector data of the south Peruvian sub-Andes. Same abreviations as on Table 1. Localizations of the sites are shown on Figure 1; data are shown on stereonets of Figure 12.

Oligo-Miocene compressional phase in the Mazuko area. The Neogene-early Quaternary Mazuko formation, at least 3000 m thick, is folded. A set of five or six Quaternary fluvial terrraces rests unconformably on the later formation. We did not observe any trace of faulting affecting these terraces. Thus, as in Quince Mil basin, the last deformations are seen to affect deposits which are attributed to early Quaternary.

Dissymetric folds associated with steeply dipping reverse faults strike approximately N100° to N110°E, and affect the Mazuko conglomerates. Vergence is toward the NE, i.e., toward the Amazonian plain. Two sites have been analyzed: one along Chiforongo river (Figure 11, site 18b) and the other one along Dos de Mayo river (Figure 11, site 18a) 2.5 km to the SSW and 3 km to the NNE of Mazuko, respectively. At Chiforongo, striated reverse and strike-slip faults were measured mainly in the clayed sands of the Mazuko formation. As in other sub-Andean localities, the bad quality of outcrops only permits estimation of the fault throws which are generally of the order of 1 m. At Dos de Mayo, striations were measured on flat sides of cobbles within a 20° dipping fold limb. They might only reflect local deformation within this fold limb without any regional significance.

Fig. 12. (opposite) Reverse strike-slip vector data from sub-Andes of south Peru used to compute solutions of Table 2 (site situations on Figures 1 and 11). Wulff stereonet, lower hemisphere. Same symbols as on Figure 4.

However, at both sites, reverse and strike-slip movements are such that they agree with roughly N-S shortening (Figure 12, sites 18a and 18b). Despite the poor quality of the data, with respect to the model hypotheses, computation gives solutions of fairly good quality (see histograms 18a and 18b, Figure 12) with a N3° trending compression at Chiforongo (18b, Table 2) and a N16° trending compression at Dos de Mayo (18a, Table 2). Thus, in the sub-Andean folds the last deformations observed are compressional and result from roughly N-S shortening.

Another example of faulting associated with sub-Andean folds is visible in the NW-SE striking Salvacion syncline (Figure 10, point 15). It is located some 100 km to the WNW of Mazuko and on the NE side of the Pongo de Conec faulted range that separates it from the Pillcopata basin. This Salvacion syncline consists of Late Cretaceous to Paleogene red beds conformably covered by gray-brown clayed sands that are interbedded upward with conglomerates. These sands and conglomerates are very similar to the Mazuko formation (Laubacher et al., 1982) and are probably also of Neogene age. The uppermost part of the Salvacion syncline consists of fluvial conglomerates that could be equivalent to the upper conglomerates of the Mazuko formation and thus could be of early Quaternary age. No unconformity has been observed in the Salvacion syncline. Nevertheless, owing to the lack of good outcrops, the relations between the uppermost conglomerates and the Neogene sands below have not been clearly observed. Strong differences of dip of the two formations could indicate

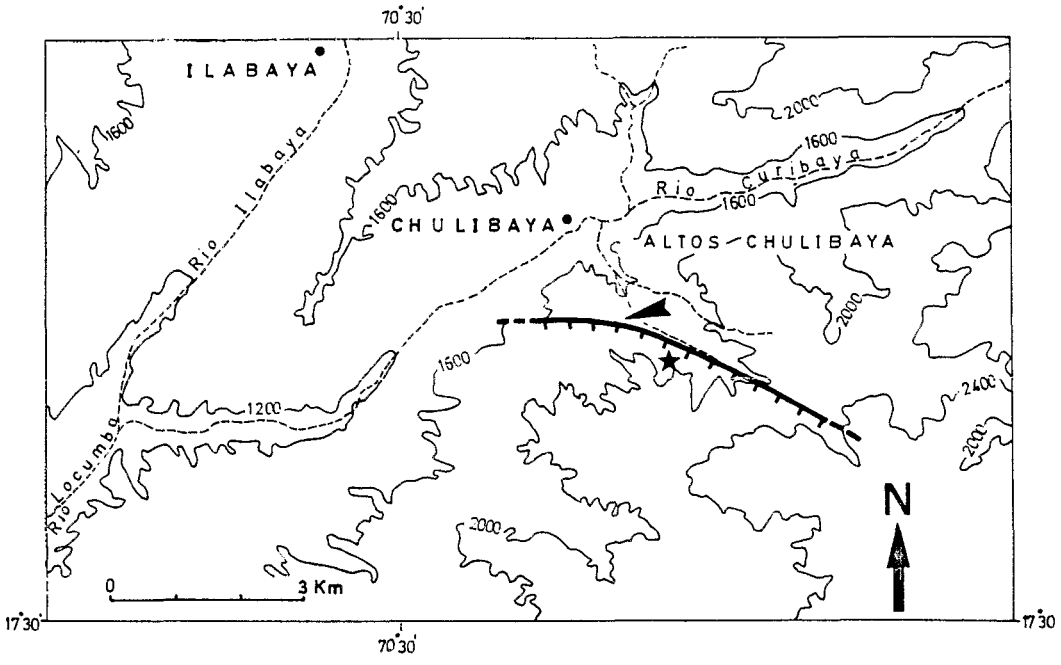

Fig. 13. Location of the Chulibaya active normal fault (Figure 1, point 7). Fault belongs to the Incapuquio fault zone (IF on Figure 1), separating the High Andes from the Pacific Lowlands. Reactivation of the fault created a south facing scarplet (thick line hatchured toward the downthrown block, see Figure 14). Chulibaya site (6-7, Figure 4) is marked by a star. Arrow head indicates location of Figure 14.

an unconformity between them. Whatever the case, the deformations of these uppermost conglomerates are the youngest that we observed in this area since no evidence of deformation has been observed in the Quaternary fluvial terraces that lie unconformably on the Salvacion syncline.

Upstream from Salvacion village, along the river, striations on flat sides of cobbles of the uppermost conglomerates have been measured within a 20° dipping fold limb (Figure 12, site 15). As in the other sub-Andean localities, these data agree with roughly N-S trending shortening. Bearing in mind the same restrictions as for the Dos de Mayo site, we processed the data with the numerical method. The obtained solution (site 15, Table 2) is of good quality (see histogram 15, Figure 12) and gives a N191° trending compression.

Slip movements deduced from striations have been measured in six sub-Andean localities situated in various structural settings: reverse faulting, thrusting associated with folding, and discontinuous deformation of fold limbs. All evidence a nearly N-S trending compression. Unfortunately, the age of this N-S trending compression is not very precisely constrained. According to Laubacher et al. (1982) it affects early Quaternary deposits. The Quaternary alluvial terraces covering them unconformably do not show any evidence of deformation. It is not known whether compressional deformation is still active, since no focal mechanisms are available in this particular south Peru segment of the sub-Andes. However, it is likely that this N-S trending compression is of early Quaternary age, as it is well known in the whole High Andes and Pacific Lowlands of Peru and Bolivia (Sébrier et al., 1982). This is also strongly supported by focal mechanisms which evidence a present-day roughly E-W direction of compression in the sub-Andes of central Peru, south Bolivia, and NW Argentina.

EXTENSIONAL TECTONICS IN THE PACIFIC LOWLANDS

Fault Zone Separating High Andes From Pacific Lowlands

From the Pacific Piedmont (Pacific Lowlands) to the Western Cordillera, the

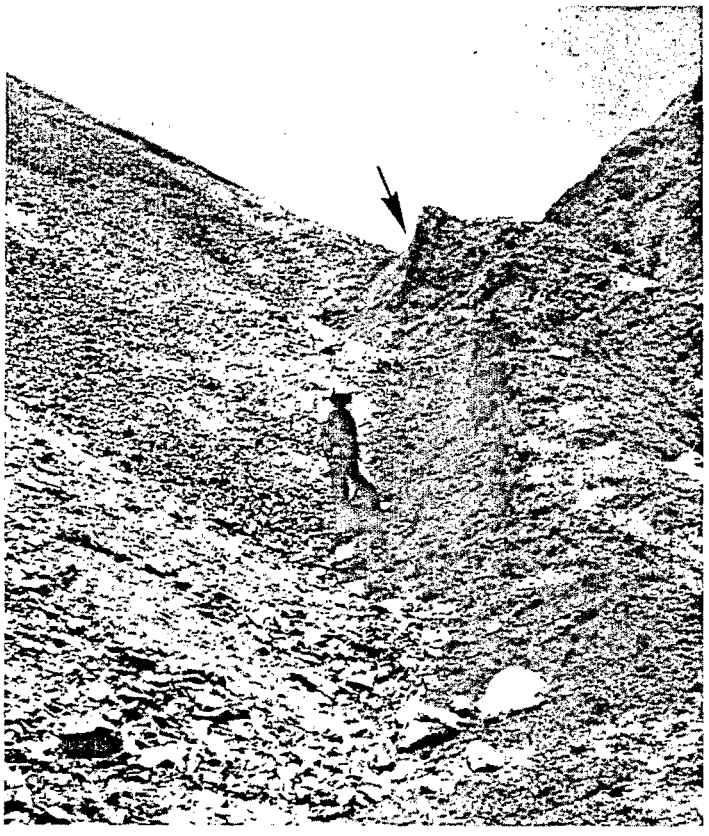

Fig. 14. Western part from the south facing scarplet (arrow) of the active Chulibaya normal fault offseting up to 2.5 m the topographic slope partly covered by screes of Holocene age (location on Figure 13).

elevation generally increases from about 2000 m up to more than 4000 m along a 20-km distance. This transitional topographic zone often coincides with a fractured belt, faults having generally a high angle dip. This fault belt results from a long tectonic history beginning in the Upper Cretaceous. Thrusts and reverse, strike-slip, and normal faults are superimposed (Vicente et al., 1979; Sébrier et al., 1979, 1982). Here, we focused our study on the active movements and on the final kinematics of the faults observed respectively in the region of Chulibaya, SE of Arequipa (Figure 1, points 6 and 7), and of Llucila, NW of Arequipa (Figure 1, point 5).

The Chulibaya active normal faults. The Chulibaya active normal fault (Figure 1, point 7) belongs to the fault belt, locally known as the Incapuquio fault zone (IF on Figure 1). It is located upstream from the Locumba river, about 2 km south of the Chulibaya hamlet (Figure 13). The fault affects the Paleocene Toquepala volcanic formation. It strikes N80°E to N120°E and dips 70° to the south.

Reactivation of the fault created a south facing scarplet (Figure 14) which offset up to 2.5 m the topographic slope partly covered by screes of Holocene age. Scarplet and opposite dipping slope form a narrow furrow. In some places, it has been filled, probably during an earthquake, by screes which do not have desert varnish comparable with the superficial screes. In other places, this furrow is underlined by puddles of dry mud which has been supplied by the last desert rainfall. In the Peruvian desert the periodicity of major rainfalls is about one or two per century (Lettau and Lettau, 1978). In the Rio Curibaya valley (Figure 13), inhabitants assert that last heavy shower occurred approximately in 1948. They do not remember any major seismic event prior to

this date, we assume that the Chulibaya normal fault has not been reactivated since at least one century.

Along the Chulibaya fault we have observed only three striated slickensides (data 1, 2, 3 on stereonet 6-7, Figure 4). They confirm the nearly pure normal component on faults having a E-W direction. At Cerro Garita (Figure 1, point 6) nearby Toquepala, 30 km to the WNW of Chulibaya, we observed five additional normal faults the striations of which correspond to the last movement along the Incapuquio fault zone (data 5-8 on stereonet 6-7, Figure 4). Kinematics of most of the faults show a N-S lengthening. The Chulibaya and Cerro Garita faults are regional faults of a comparable magnitude, and we have assumed therefore that the deformation, in the region under consideration, is homogeneous enough to process the data together. The obtained solution (6-7, Table 1) gives a N3°W striking extension σ 3. This solution is of good quality for the two sets of data, the angles (t,S) being lesser than 10° for all the data (see histogram 6-7, Figure 4). However, the obtained solution is not strongly constrained due to the orientations of the fault planes which are not well distributed. The kinematics of the active normal Chulibaya fault is in agreement with a NS trending extension.

The normal movement on the Llucl1a fault. The Llucl1a fault (Figure 1, point 5) is located in the Rio Sihuas valley, 60 km to the WNW of the city of Arequipa. It limits the Precambrian rocks of the Western Cordillera from the Oligo-Miocene continental deposits of the Pacific Piedmont (Figure 15). This fault zone, which occupies the same structural situation as that of the Incapuquio fault zone (Figure 1, points 6 and 7), also exhibits a complex tectonic history. On the major fault planes the most important movements result from reverse strike-slip or reverse slip. Normal and normal strike slip striations (Figure 4, site 5) postdate the above compressional deformations and appear to result from the last period of activity of the fault zone. Unfortunately, at Llucl1a this extensional tectonics is not precisely dated. It is younger than the compressional structures which deformed the Oligo-Miocene deposits (Moquegua formation). On the other hand, the lack of morphological scarplet seems to indicate that it is prior to the Holocene. Thus this extensional tectonics could be of Pliocene-Pleistocene age.

The 16 normal striations of the ultimate period of activity are in agreement with a N-S lengthening (Figure 4, site 5). Computation has been performed with these data. The obtained solution (5, Table 1) gives a N14°E striking "extension" σ 3; this solution is of good quality, as 15 striations have (t, S) angle lesser than 20° (see histogram 5, Figure 4).

Thus the youngest reactivations of the Llucl1a fault and of the Incapuquio fault zone, both of which limit the Western Cordillera from the Pacific Lowlands, appear to result from a N-S trending extensional tectonics. The N140°E trending, 70° south dipping Pampacolca fault, located 60 km to the NW of Llucl1a on the same fault belt (PF on Figure 1), has probably been reactivated by this N-S extension as it offsets early Quaternary alluvial fans and shows a normal throw of some 20 m. However, its kinematics has not been studied in more detail due to unfavorable outcrops.

The Normal Faults Along the Pacific Coast

The coastal area of south Peru lies above a zone of high seismicity which occurs either at the contact between the oceanic and continental plates or within the oceanic slab. In contrast, few seismic foci are clearly located within the continental wedge of the overriding plate, and they have not provided focal mechanisms. The interplate earthquakes are characterized by thrust-type focal mechanisms, whereas the foci located within the oceanic slab show normal faulting mechanisms (Stauder, 1973, 1975; Isacks and Barazangi, 1977; Malgrange et al., 1981; Chinn and Isacks, 1983). Microseismic data obtained from local networks do not indicate such a simple pattern (Grange et al., 1984b), normal, reverse, and strike-slip faults not being clearly separated in space. Moreover, a double-layered Benioff zone is not observed in southern Peru (Bevis and Isacks, 1984).

Many Quaternary faults with normal throws have been reported all along the Pacific coast (Lavenu and Soulas, 1976). Our observations confirm that the Quaternary and Recent tectonics is characterized by normal faults whose extension is of small magnitude, throws being always less than few meters. We have

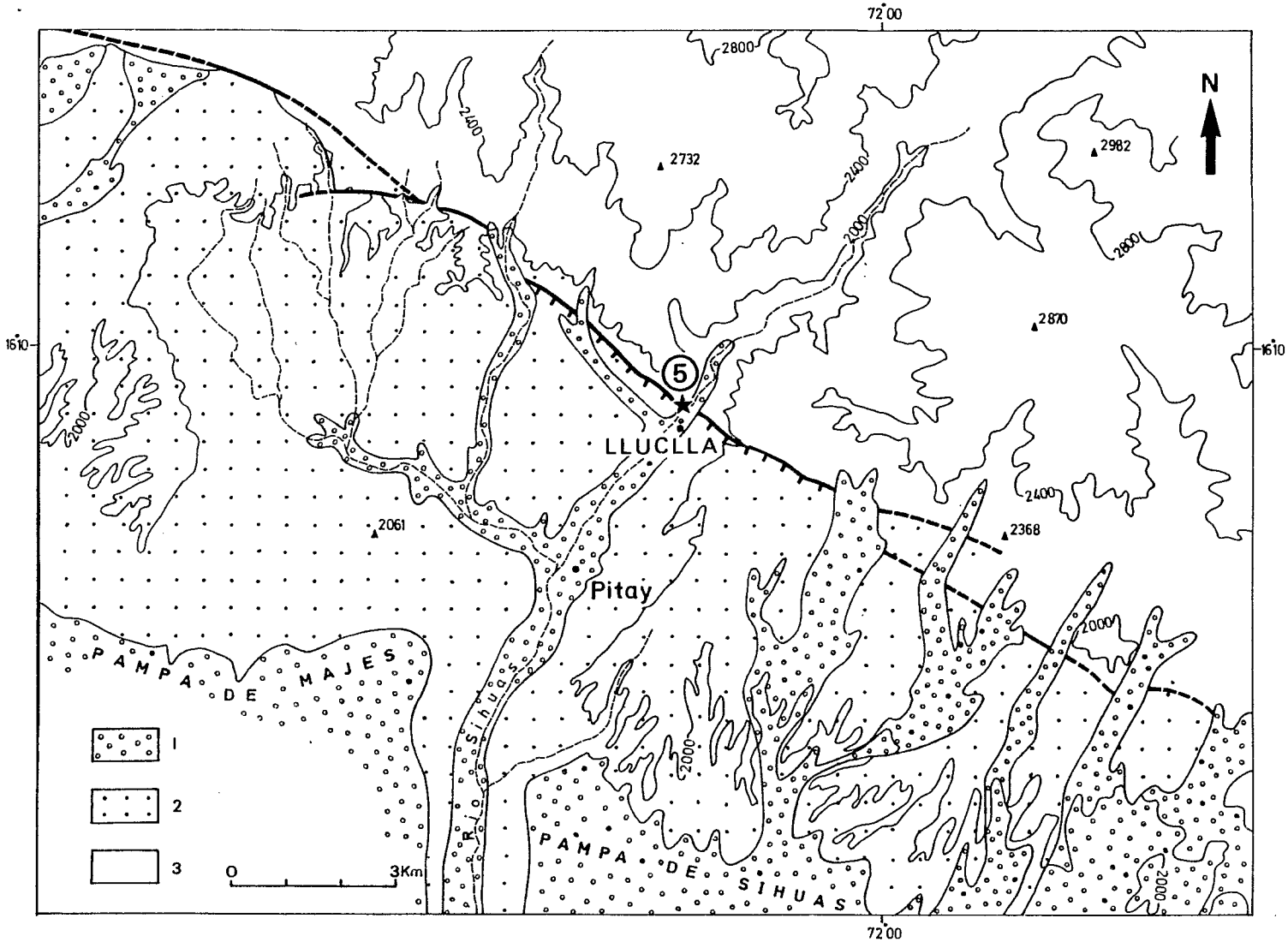

Fig. 15. Structural sketch of the Lluclla fault (Figure 1, point 5). Normal movements of the fault (hatchured toward the downthrown block), postdating compressional deformations, are not precisely dated but could be of Plio-Pleistocene age. 1, Plio-Pleistocene continental deposits; 2, Oligo-Miocene deposits (Moquegua formation); 3, Precambrian rocks of the Western Cordillera intruded by the coastal batholith. Solid star (number 5) indicates the Lluclla site.

Fig. 16. Near San Juan de Marcona (point 1a, Figure 1), Quaternary marine terrace (Q) overlies unconformably Pliocene marine beds (P). Photograph shows a N120°E striking normal fault (F, normal movement indicated by thick arrows) with a small 0.5-m downthrow (see datum 1 on stereonet 1, Figure 4). The steep, or slightly overturned, dip of the curved fault plane seen near the surface is related to the upward decrease of the vertical load in poorly consolidated sediments. This gives an apparent reverse fault geometry (F with thin arrows) on the surface (north right).

also observed some reverse faults, but they are generally due to early Quaternary compression. However, some small reverse faults with offsets less than few meters affect middle Quaternary formations near Tacna and Chincha (Figure 1). Unfortunately, field evidence is not clearly demonstrative. If they were of tectonic origin, this should mean that at the surface along the coast the Recent state of stress fluctuates around a neutral position but with a preferential extensional regime of small magnitude. Although Quaternary normal faults have been reported in many places along the Pacific coast (Lavenu and Soulas, 1976),

striated fault planes have been observed only at four localities: Marcona (point 1), Chala (point 2), Calaveritas (point 3), and La Planchada (point 4, Figure 1).

Normal faulting along the Pacific coast opposite the Nazca ridge (the Marcona area). The Marcona area is located on the Pacific coast, opposite the aseismic Nazca ridge (Figure 1, point 1). A set of Quaternary stepped marine terraces is well developed in this area, the oldest being at an altitude of 700 m (Legault, 1963). They lie unconformably on Pliocene marine beds (Sébrier and de Muizon, 1982). In this area the most recent faults are normal with throws ranging between several decimeters and several meters. They postdate compressional deformations which affect the Pliocene marine beds. Moreover, some of them offset Quaternary marine terraces (Figure 16). Unfortunately, owing to the sandy nature of the material, the normal fault planes do not exhibit striations that could indicate the slip vectors.

In the Marcona area we observed only eight normal striated fault planes. Two were measured at San Juan de Marcona harbor (Figure 1, point 1a) where a fresh roadcut shows normal faults offseting a marine, upper Pleistocene terrace. Five other slickensides were measured at Alto Grande (Figure 1, point 1b), 30 km to the ESE of San Juan and one at Aguada de Lomas (Figure 1, point 1c), 7 km SE of Alto Grande. They show clearly a north to NE striking lenthening (Figure 4, site 1). This is in agreement with the occurrence in the Marcona area of numerous nonstriated Quaternary normal faults which have a roughly E-W direction (Lavenu and Soulas, 1976).

A poorly constrained result should be expected from computation of these eight measured slickensides since data are few and spread over a large area. However, we have processed them assuming that the tensional deformation is sufficiently homogeneous in view of the scale of the study and because of the widespread E-W normal faults which occur over the whole area. The obtained solution (1, Table 1 and Figure 4) gives a N12° striking "extension" σ 3. In the Marcona area the youngest Quaternary tectonics is extensional and is characterized, as in other south Peruvian localities, by a roughly N-S tensional direction.

Normal faulting on the Pacific coast south of Nazca area. South of 15°40'S, the Coastal Cordillera 1000- to 1300-m-high scarp faces the Pacific Ocean. This south facing major scarp is the result of movements on a major fault zone limiting the marine forearc basins from the Pacific Lowlands. This fault zone does not outcrop clearly on land and seems to be mainly located offshore. The coastal scarp is notched by marine terraces of upper Oligocene to upper Quaternary age (Sébrier et al., 1979; Huaman, 1985), and this kilometric scarp is mainly inherited from the Oligo-Miocene tectonics. Unfortunately, Tertiary, and moreover Quaternary, deposits are scarce so that Quaternary movements on the above-mentioned fault zone are not precisely known; it can only be stressed that all the observed faults show small displacements.

The Chala faults: Chala Bay (Figure 1, point 2) is located about 100 km ESE of San Juan de Marcona. A set of Quaternary stepped marine terraces, the highest reaching an altitude of 250 m, outcrops around the bay (Laharie, 1970). They lie unconformably on Tertiary marine beds. As in the Marcona area, the youngest Quaternary deformation that we observed is characterized by small normal faults, whose planes generally do not exhibit striations. We measured only three striated slickensides that cut upper Pliocene to early Quaternary sandy clay marine deposits located on the western part of Chala Bay. They include a SW block downthrown several decimeters and show a normal sinistral movement (data 2: 1, 2, 3, Figure 4, A). These three data do not permit computation of the extensional direction but are in agreement with a roughly N-S lengthening.

The Calaveritas and La Planchada faults: The upper Pliocene marine beds of the La Planchada formation outcrop on both sides of the mouth of the Rio Pescadores (Figure 1, points 3 and 4) (Beaudet et al., 1976). These formations exhibit several superimposed deformations: (1) normal faults contemporaneous with Pliocene sedimentation, (2) compressional deformations, and (3) normal faults which cut deformations 1 and 2. At Calaveritas (Figure 1, point 3) and La Planchada (Figure 1, point 4) we have measured two striated normal fault planes (data 3-1 and 4-1, Figure 4, A) whose NE block is downthrown several decimeters. Although these are small, they show that in this area, kinematics of the Quaternary normal

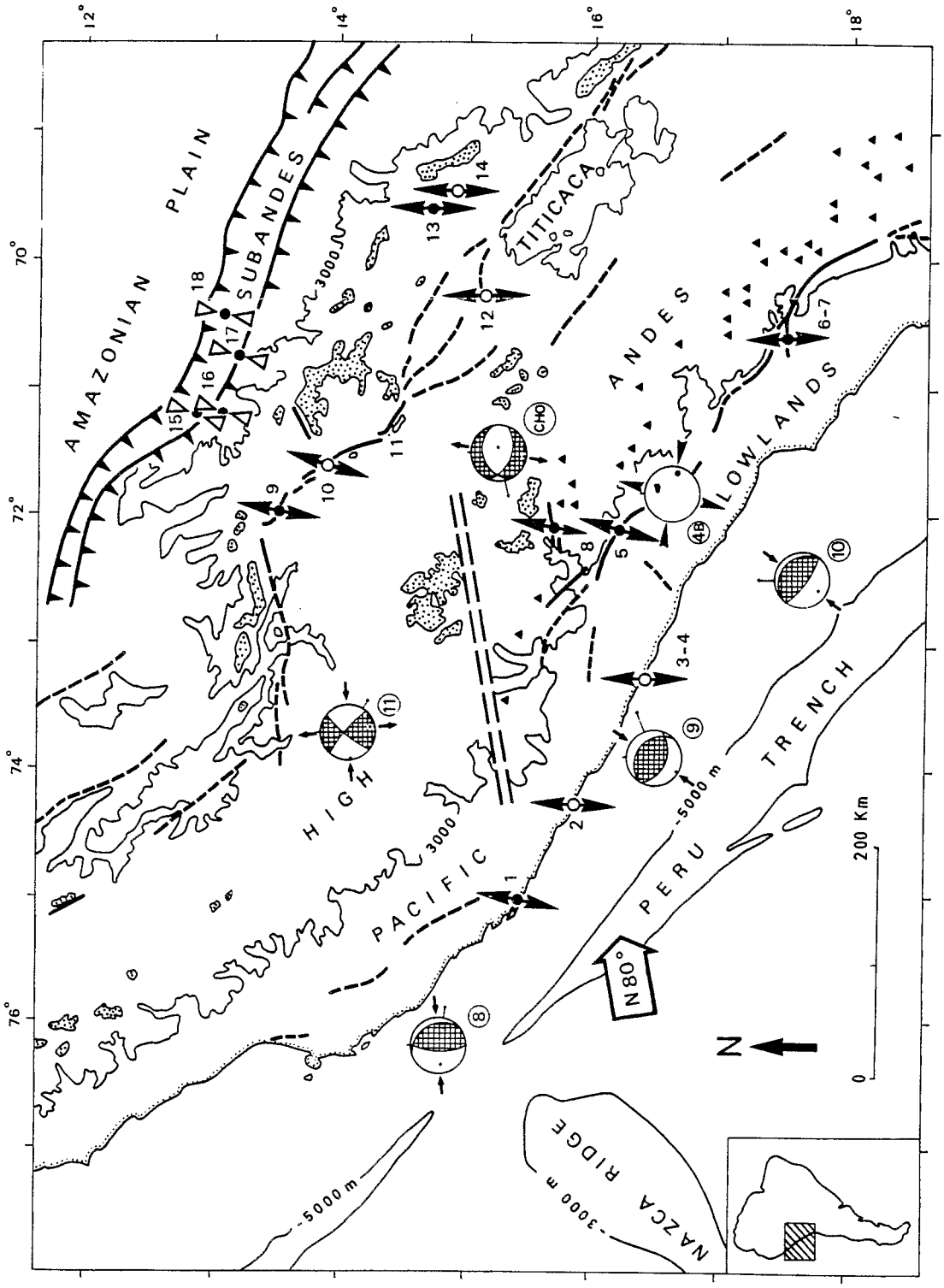
12°
14°
16°
18°
70°
72°
74°
76°
AMAZONIAN PLAIN
SUBANDES
TITICACA
ANDES
LOWLANDS
HIGH
PACIFIC
PERU TRENCH
-5000 m
-3000 m
3000
N80°
200 Km
0
N
NAZCA RIDGE
CHO

Fig. 17. Principal directions of extension and compression deduced from structural analysis of Quaternary and active faults of the Andes of south Peru. Arrows attached to open circles are for graphical solutions and to solid circles for computed solutions. In Pacific Lowlands and High Andes, N-S striking, regional extensional direction appears to be roughly orthogonal to the direction of convergence (large white arrow) between the two plates (Minster et al., 1974; Minster and Jordan, 1978). In sub-Andes, σ 1 (compression) principal stress directions strike roughly N-S (convergent. open triangles). As discussed in the text, N-S trending shortening seems to be of early Quaternary age, while the present-day compression strike roughly E-W. The 3000-m lines separate the High Andes from lowlands, stippled areas have an altitude higher than 5000 m. (Numbered sites as in Figure 1). Available focal mechanisms (arrows indicate direction of P or T axes) at the contact between the Nazca and South American plates are circled 8, 9, and 10; same numbers as from Stauder (1975) and Chinn and Isacks (1983). Circled 11 (Suarez et al., 1983) is a superficial crustal event (depth 8 km). CHO (Chonta) is a composite focal mechanism of small crustal superficial events (Grange, 1983); 4B gives directions of extension (divergent arrow heads) and compression (convergent arrow heads) deduced from 10 focal mechanisms of small events (Grange, 1983) at depths ranging between 12 and 40 km (see Figure 4). Double thick dashed line is the vertical projection of the transition zone between flat dipping slab to the north and the 30° dipping slab to the south (Grange et al., 1984b).

faults is in agreement with the general N-S lenghening (Figure 4, A) visible in the Pacific Lowlands.

QUATERNARY AND RECENT STATE OF STRESS IN THE ANDES OF SOUTHERN PERU

Quaternary Faulting, Focal Mechanisms, and State of Stress in Andes of Southern Peru

Within the Andes of southern Peru, Bolivia, and north Argentina-Chile, which are situated above a 30° east dipping slab, seismicity is moderately active along the sub-Andes. No focal mechanisms have been published for the south Peruvian sub-Andes. Sub-Andes of south Peru are clearly affected by compressional tectonics (Laubacher et al., 1982). Structural analysis of folds and faults affecting early Quaternary alluvial deposits shows a roughly N-S shortening (Figures 12 and 17). Is this N-S shortening the result of the early Quaternary compression as known in many places of the Andes of Peru (Sébrier et al., 1982), or is it the direction of late Quaternary-Recent shortening, the strike of which would have been induced by the inherited N120°E orientation of the sub-Andes of south Peru and north Bolivia? The poor quality of outcrops in the Amazonian forest does not permit structural analysis in the Recent Quaternary deposits. Comparison with the Recent state of stress in the Andes of central Peru (M. Sébrier et al., manuscript in preparation, 1985) argues in favor of the first proposition. In central Peru the stress pattern is similar to that of south Peru (Figure 17). N-S trending extension prevails in the High Andes, and the last compressional structures affecting early Quaternary formations in the sub-Andes result from N-S compression as in south Peru. However, focal mechanisms in the central Peruvian sub-Andes (Stauder, 1975; Suarez et al., 1983) show that the active compression strikes roughly E-W. In addition, focal mechanisms in sub-Andes of south Bolivia and NW Argentina (Chinn and Isacks, 1983; Jordan et al., 1983) also show E-W striking compression. This strongly supports the fact that in south Peru as in central Peru N-S compression in sub-Andes is of early Quaternary age and that active compression strikes E-W.

In the High Andes and Pacific Lowlands, the youngest Quaternary deformations

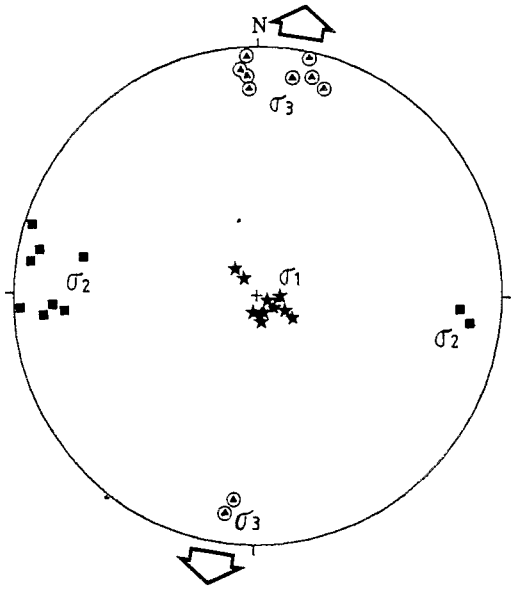

Fig. 18. Principal stress direction computed from slip vectors of Quaternary and Recent normal faults of the High Andes and Pacific Lowlands of south Peru. Recent Quaternary faulting in these regions results from a state of stress such as σ 1 (compressional axis) is vertical and σ 3 ("tensional" axis) strikes between N5°W and N18°E.

clearly result from normal and normal strike-slip faulting. The major faults which are presented in this paper (Cuzco-Tambomachay, Vilcanota, Huambo-Cabana Conde, Chulibaya, etc., faults) have lengths ranging between 5 and 20 km. Cumulative Quaternary normal throws are generally greater than 100 m. Moreover, these faults are seen both in Quaternary deposits and in bedrock of Precambrian to lower Tertiary age. Clearly, their kinematics are not controlled by landslide effects. Where Quaternary faults are of smaller magnitudes and/or are observed only in poorly consolidated Quaternary sediments, their kinematics is in agreement with the N-S extension deduced from analysis of the major faults. In the Western Cordillera, recent normal faulting is contemporaneous with volcanic activity. Thus it appears reasonable that the normal Quaternary faults described in this paper are not the result of surface effects such as landslides but are representative of the state of stress at least in the upper part of the crust of the High Andes and Pacific Lowlands.

Analysis of the exposed striations permits datermination of the slip vectors of these normal faults. Computations performed on 81 striated fault planes from six different areas show that the recent deformations result from a state of stress (Figure 18), such as the minimum principal stress (σ 3) that strikes roughly N-S, the intermediate principal stress (σ 2) E-W, whereas the maximum principal stress (σ 1) is nearly vertical (Table 1 and Figures 17 and 18). The stress ratio

TABLE 3. Data Used to Estimate the Magnitude of Stretching Produced by N-S Trending Extension in the High Andes and Pacific Lowlands along the 72° Meridian Between Cuzco and Mollendo-Southern Peru

	S, deg	D, deg	P, deg	Tv, m	X, m
EC	N 90	55	85	200	140
CZ	N 120	50	75	400	361
WC	N 100	55	80	400	315
IF	N 120	65	70	200	121
PC	N 120	60	75	500	330
					1267
					0.3%

Middle to Recent Quaternary deposits being untilted, it is supposed that no rotation of the fault planes has occurred. Stretching (X) may be calculated for each fault using estimate vertical throw (Tv), mean dip (D), mean fault strike (S), and the mean striation pitch (P). Subsequently, N-S components of stretching for each fault have to be added along the N-S section: $X = Tv/\sin D(-\cos S/\tan P+\sin S.\cos D)$. Data are taken from the Ananea basin (13), Eastern Cordillera (EC); from Tambomachay fault (9), Cuzco basin (CZ); from Trigal and Solarpampa faults (8), the Western Cordillera (WC); from the Incapuquio fault (6), (IF) and from Marcona area (1, Figure 1), Pacific Coast (PC), the mean throw being estimated from the maximum elevation of Quaternary marine terraces. These data indicate that stretching between Cuzco and Mollendo along the N-S trending, 400-km-long section has a value of 0.3%. Study of faults has been discontinuous along this section. We have supposed that stretching due to small unsurveyed faults might be of the same order as stretching due to the major faults. Thus total stretching is probably of the order of 1% for the last 1 or 2 m.y.

($R=\sigma'2-\sigma'1/\sigma'3-\sigma'1$) has values ranging between 0.4 and 0.8. This implies that the minimum ("tensional") principal axis σ 3 is clearly different from the intermediate one σ 2 and thus well determined with respect to the last one. A similar result is obtained from graphical analysis of 12 additional striated fault planes from six other localities (Figure 4, A). Thus 93 striated normal fault planes demonstrate a N-S trending tensional tectonics of Quaternary age.

As mentioned above, the south Peruvian Quaternary normal faults are either still active, offset Quaternary deposits, or postdate compressional structures which affect Pliocene and early Quaternary formations. The few radiometric dates of Peruvian Quaternary units do not permit precise determination of the time duration of the N-S trending tensional tectonics. This depends mainly of the accurate dating of the early Quaternary compressional tectonics. In the central Andes, two compressional episodes are observed (Lavenu et al., 1980; Mercier, 1981; Lavenu, 1981; Sébrier et al., 1982). They probably occurred between about 2 and 3 m.y. B.P.: on one hand, they are younger than dated late Pliocene beds and conglomeratic deposits assigned to the early Quaternary (Sébrier et al., 1982); on the other hand, they are older than several Quaternary units of assumed early to late Quaternary ages. Hence according to the presently available data the Quaternary tensional tectonics seems to have been active during the last 1 or 2 m.y. We estimate the horizontal stretching produced by Quaternary extension along the 72°W meridian line. This calculation (see Table 3) is obviously a rough approximation and gives only an order of magnitude which appears to be less than 1%. Therefore the Quaternary N-S stretching is very small and cannot be compared with extension reported either in back arc spreading settings or in the intracontinental Basin and Range province.

Within the Western and eastern Cordilleras, no teleseimic focal mechanisms are available. In the Western Cordillera, near Chonta (CHO in circle on Figure 17), a composite focal mechanism of poor quality according to Grange (1983) and Grange et al. (1984b) has been determined from a local seismic network. It is in agreement with N-S trending extension. Beneath the High Plateau of south central Peru (Stauder, 1975; Suarez et al., 1983) one focal mechanism (11 in circle on Figure 17) shows strike-slip faulting with a N-S striking T axis and a E-W P axis. This earthquake is located within the transitional zone between the 30° dipping segment and the flat subducting segment of central Peru. The Altiplano-Puna, above the 30° dipping slab, is almost aseismic, suggesting that the mechanical state is nearly neutral (Jordan et al., 1983). In the south Peruvian High Andes, geological observations clearly testify an extensional state of stress (σ 1 vertical, N-S σ 3 and E-W σ 2 being horizontal), but the magnitude of extensional deformation is very small. A similar state of stress has been suggested on the Bolivian Altiplano (Lavenu, 1978).

Below the Pacific Lowlands of south Peru, the focal depths calculated from teleseismic data are not accurately determined. Thus focal mechanisms are not clearly related to the deformation of the upper plate, of the downgoing slab, or of the interface between the two plates. From a local seismic network, two groups of focal mechanisms have been determined (Grange, 1983; Grange et al., 1984b). Beneath the coast at a depth shallower than 55 km, they show a complex pattern of normal, strike-slip, and reverse faulting which has not been explained. Under the transitional zone between the Pacific Piedmont and the Western Cordillera, at depths ranging between 12 and 40 km, normal, reverse, and strike-slip fault solutions are more homogeneous. They are in agreement with a N105°E striking compression (Figure 4, B, and 4B in circle on Figure 17). Direction of extension is not strongly constrained, being in a plane normal to the compressional direction, and possibly dips gently toward the NNE (Figure 4, B). If correct, the state of stress is such that σ 2 is vertical, and σ 3 striking N20° to 30°E and σ 1 striking N105°E are horizontal. Whatever the case, this state of stress is clearly different from that observed at the surface (see Figure 17) in the whole Pacific Lowlands (vertical σ 1, σ 3 striking N-S and σ 2 striking E-W being horizontal). This will be discussed in the next section.

Available offshore data from the Peruvian margin (Johnson and Ness, 1981) seem to demonstrate extensional tectonics but do not provide any evidence of a N-S extension. Along the Peru-Chile trench, compressional structures have been

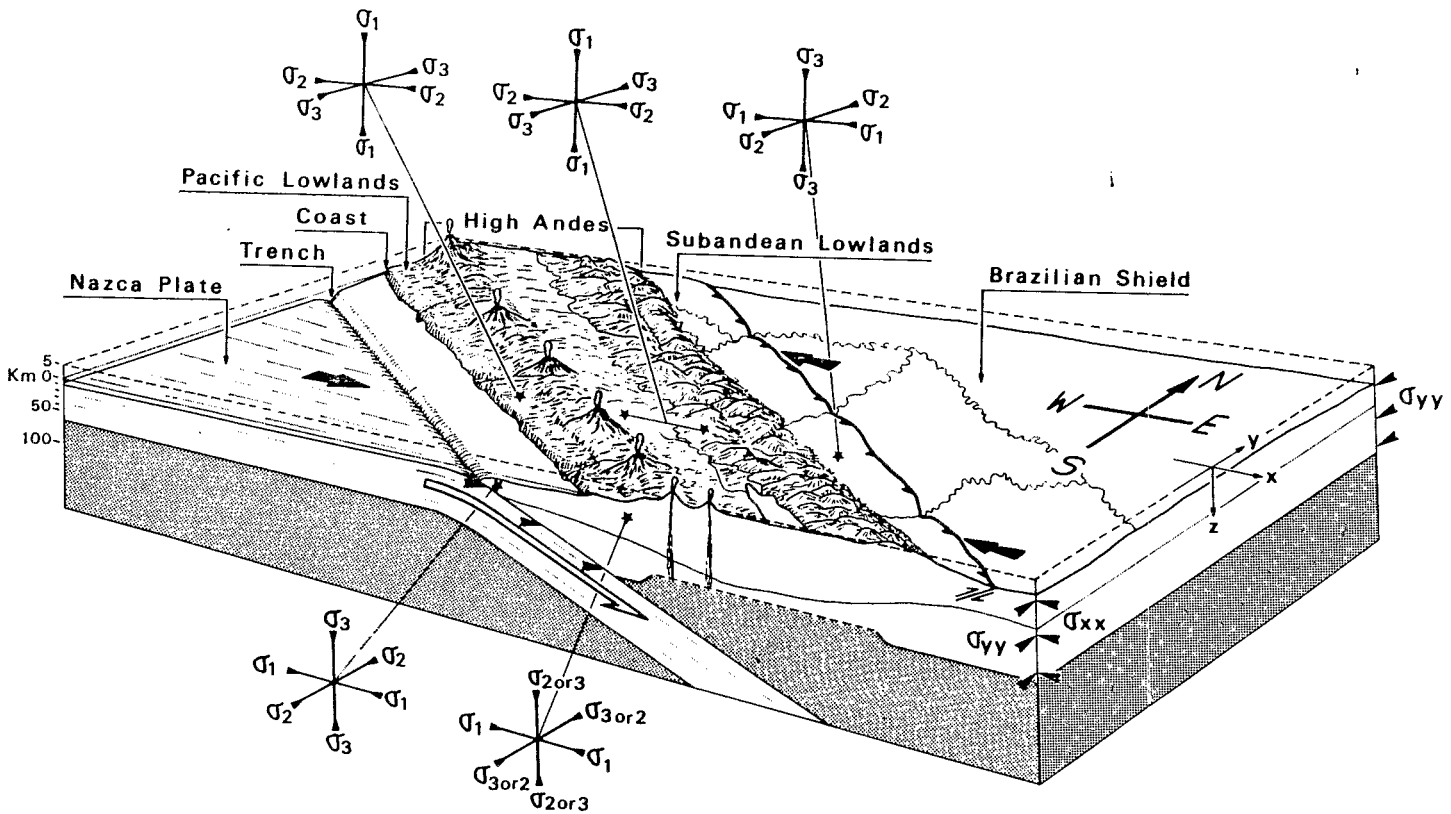

Fig. 19. Tentative model to explain the state of stress in the Andes of southern Peru. Principal average lithospheric stress (sets of thin solid arrows) in excess to the reference (sea level) lithostatic stress are σ xx (striking E-W), σ yy (striking N-S), and σ zz (vertical); σ xx and σ yy are considered as fairly constant; σ zz amount to the weight of the topography. Convergence between Nazca and South American plates (thick arrows) is roughly parallel to σ xx. In the sub-Andes, tectonics is compressional (σ xx>σ yy>σ zz), i.e., σ 3 is vertical and σ 1 is horizontal. A similar state of stress is inferred from focal mechanisms at the contact between the two plates. In the High Andes, σ zz increases, then σ zz>σ xx>σ yy; i.e., σ 1 is vertical, σ xx becomes σ 2, σ 3 strikes N-S. In the Pacific Lowlands, according to the model, tectonics should be compressional. However, at the surface, N-S extension prevails, indicating a decrease of σ xx value possibly related to the topographic effect of the deep oceanic trench. At depth, focal mechanisms indicate an E-W striking σ 1 principal stress, the vertical principal stress being σ 2 or σ 3.

described (Schweller et al., 1981) and few thrust-type focal mechanisms from earthquakes located at the contact between the Nazca and South American plates show an E-W to NE-SW direction of P axes (Stauder, 1975; Chinn and Isacks, 1983) (see circled 8, 9, and 10 on Figure 17).

The state of stress deduced from structural analysis of Recent-Quaternary faults and from few focal mechanisms is shown on Figure 17. The High Andes and Pacific Lowlands where tensional tectonics occurs are bounded by two zones of compressional deformation: the sub-Andes to the east and the Peru-Chile trench to the west.

The state of stress in the Andes of southern Peru and the effect of high topography. In regions where crustal thickening is present, extensional tectonics has been related to the effect of high topography (Tapponnier and Molnar, 1976; Molnar and Tapponnier, 1978; Dalmayrac and Molnar, 1981; Cross and Pilger, 1982; Suarez et al., 1983; Froidevaux and Isacks, 1984). Topographic features of large lateral extent are compensated at depth by mass deficiencies (isostasy). The latter, crustal root and/or hot asthenospheric material, are buoyant. The first-order effect of such a large-scale mass distribution is to perturb the vertical lithospheric stress. The average lithospheric vertical stress σ zz in excess to the reference (sea level) lithostatic stress amounts to the weight of the topography. The excess average lithospheric horizontal stress σ xx is considered to be fairly constant, the shear stress underneath the plate being neglected (Dalmayrac and Molnar, 1981; Froidevaux and Isacks, 1984). Then in lowlands, if tectonics is compressional, σ xx>σ zz, so that σ 1 is horizontal and σ 3 vertical. In regions of high topography, σ zz increases and may exceed σ xx, so that σ 3 becomes horizontal and σ 1 vertical; tectonics is extensional. Such a two-dimensional analysis could imply that direction of extension in regions of high topography has to be parallel to direction of compression in lowlands. That is supposed in Dalmayrac and Molnar s' analysis of the state of stress in central Peru; extension in Cordillera Blanca is presumed to strike roughly parallel to compression in the sub-Andes.

Structural analysis of recent Quaternary faults of south Peru shows that the "extensional" σ 3 direction strikes between N5°W and N18°E (Figure 18). The same N-S extension has also been demonstrated in Cordillera Blanca (Mercier and Sébrier, 1981; Bonnot, 1984). On the other hand, as discussed above, where compressional direction has been demonstrated in the Andean crust by focal mechanisms, it strikes roughly E-W. Therefore a three-dimensional approach must be investigated. Here (Figure 19) the principal average lithospheric stresses in excess to the reference (sea level) lithostatic stress are named σ xx (horizontal, striking E-W), σ yy (horizontal, striking N-S), and σ zz (vertical). Focal mechanisms and structural analysis of recent Quaternary faults in both southern Peru and central Peru show that σ xx is always the horizontal maximum principal stress (σ Hmax) and σ yy the minimum one (σ Hmin). In the sub-Andes, tectonics is compressional. The state of stress is defined by the relation: σ xx>σ yy>σ zz; thus σ 3 is vertical and σ 1 horizontal and, as discussed above, probably strikes E-W. In the High Andes, σ zz increases with elevation of the topography. Two states of stress are possible; they are defined by relations σ xx>σ zz>σ yy or σ zz>σ xx>σ yy. According to our observations the last state of stress prevails in the High Andes, i.e., σ 1 is vertical; whereas σ 3 striking N-S and σ 2 striking E-W are both horizontal (Figure 17). Whatever the case, σ 3 lies along the y direction and thus strikes N-S. In the Andes of southern Peru, convergence between the Nazca and South American plates (Minster et al., 1974; Minster and Jordan, 1978) is roughly parallel to σ xx, and thus extension in the South Andes is roughly orthogonal to the convergence (Figure 19).

In a general manner, in high plateaus which are submitted to lateral compression, if extension occurs due to the weight of the high topography, extensional direction must be roughly orthogonal to strongest compressional directions in the adjacent lowlands. This appears clearly on the Tibetan plateau (Molnar and Tapponnier, 1978; Tapponnier et al., 1981; Armijo et al., 1984; Mercier et al., 1984). However, along arcuate systems, compression along boundaries is not necessary parallel to convergence as it is the case in the Andes. It is noteworthy that away from the convergence

zone, σ xx trajectories may be deflected due to possibilities of lateral flowing of the crustal material (Tapponnier and Molnar, 1976). Principal deviatoric stress values may vary along the same σ xx trajectory so that successive σ'1, σ'2, σ'3 deviatoric values may be present along this trajectory, as demonstrated in Asia (Tapponnier and Molnar, 1976, 1979), in the Aegean arc (Mercier et al., 1979; Mercier, 1981), and in the Japan arc (Nakamura and Uyeda, 1980). In the Andes the successive σ'1 (in the sub-Andes) and σ'2 (in the High Andes) deviatoric values along the σ xx trajectory reveal the increase of σ zz due to the high topography in comparison with σ Hmax.

Such a model does not explain the state of stress in the Pacific Lowlands, where the state of stress is nearly neutral but with a preferential tendency to N-S extension. Many authors (Sacks et al., 1978; Cross and Pilger, 1982; Froidevaux and Isacks, 1984) have proposed that extensional deformation may be due to flexion of the continental plate along the convergence boundary (Figure 19). Above the neutral surface of the plate, traction should occur and σ xx decreases. If σ xx becomes smaller than σ zz but remains higher than σ yy, then N-S extension may occur. However, bending might be roughly parallel to the N120°E striking coast, and thus extension above the neutral surface should be orientated roughly N30°E and not along the σ xx direction (N80°E). D. Mc Kenzie (personal communication, 1985) has suggested that decreasing of σ xx along the Pacific coast may be due to a topographic effect related to the nearby 7000-m-deep trench.

Finally, on high plateaus with crustal thickening, as the Andes, extension roughly parallel to the convergence must result from a state of stress clearly different from the present-day one. It is defined by the relation $\sigma xx < \sigma yy < \sigma zz$. Such a state of stress implies that forces applied to a convergence boundary drastically decrease. Along subduction zones, several geodynamic processes may be put forward to explain such a situation (see Cross and Pilger, 1982), for instance, seaward migration of the slab, slow or retrograde absolute movement of the upper plate which allows seaward migration of the trench. Whatever the situation, the high plateau is no longer laterally sustained and flows toward the trench. This is the Mariana-type arc of Uyeda and Kanamori (1979), and Uyeda (1981, 1982).

Extensional Tectonics in Andean Convergent Zone Versus Benioff Dip

There is now a general agreement on the configuration of the Andean Benioff zone. It dips with an angle of 30° to the east or northeast beneath the Altiplano (between latitude 15°S and 28°S) and central Chile (south of latitude 33 S), where active volcanism occurs. On the contrary, it is rather flat beneath central Peru (north of latitude 15°S) and north central Chile (between latitude 28° S and 33° S), where no active volcanism is known (Stauder, 1973; Barazangi and Isacks, 1976). The sub-Andean zone is wider and seismically more active above the flat subduction segments than above the steeper subduction ones (Jordan et al., 1983). Mégard and Philip (1976) proposed that the recent and active deformations of the overriding plate should be compressional over the flat Benioff segments and tensional over the steeper ones. However, Quaternary extension also occurs in central Peru but seems to be restricted to the Coastal Lowlands and Western Cordillera (e.g., Cordillera Blanca) areas, whereas compression extends in the whole Eastern Cordillera and sub-Andes (Sébrier et al., 1982). Thus tensional tectonics affects a narrower zone in central Peru than in southern Peru. Therefore there seems to exist a correlation between the spatial occurrence of tensional/compressional tectonics and the geometry of the underlying subduction zone. As commonly accepted (Barazangi and Isacks, 1976; Cross and Pilger, 1982) where the subduction flattens, the coupling between the Nazca and the South America plates increases. Consequently, σ xx has a higher magnitude, and compression plays a more important role in the overriding continental lithosphere. On the contrary, where the oceanic slab dips steeper, an asthenospheric wedge appears, causing volcanism to occur (Barazangi and Isacks, 1976). In addition, coupling between the two plates becomes weaker so that extensional domain affecting the High Andes is more extensive. This latter case is illustrated by the present-day state of stress in southern Peru. It is noteworthy that during Neogene and early Quaternary, compressional deformations have affected

the whole central Andes, highlands and lowlands (Dalmayrac and Mattauer, 1980; Martinez, 1980; Sébrier et al., 1980b; Mercier, 1981; Megard et al., 1984). These observations probably imply a strong increase of σ xx value which indicates that geodynamic conditions were different from present ones.

CONCLUSIONS

Field studies in south Peru clearly show (Figure 17) the following:

1. In the sub-Andes, deformations are compressional. They have been observed affecting Neogene and early Quaternary deposits and reflect a roughly N-S striking compression. Unfortunately, the poor quality of outcrops in the Amazonian forest does not permit structural analysis of the Recent Quaternary deposits. However, as largely discussed in this paper, this N-S compression is more likely the early Quaternary direction of compression rather than the present-day one. This latter probably strikes E-W as shown by focal mechanisms in the sub-Andes of central Peru, South Bolivia, and NW Argentina.
2. In the High Andes, Recent and active deformations result from normal faulting. Several faults have lengths ranging between 5 and 20 km and are seen both in the bedrock and in Quaternary formations. Their kinematics illustrate a N-S striking extension. However, magnitude of stretching is small, of the order of 1%.
3. In the Pacific Lowlands, Quaternary normal faults also result from N-S trending extension whose magnitude appears to be smaller than in the High Andes.

Structural analyses of faults and some focal mechanisms enable us to propose a sketch of the state of stress in the Andes of south Peru. High Andes and Pacific Lowlands are affected by N-S trending extension. They are bounded by two zones of roughly E-W striking compression: the sub-Andes to the NE and the contact between the Nazca and South American plates to the SW.

In such a sketch (Figure 19), σ Hmax trajectories strike E-W and thus are roughly parallel to the convergence direction; σ Hmax is σ 1 in the sub-Andes, and at the contact between the two plates, σ Hmax is σ 2 in the High Andes. Thus σ Hmin strikes N-S; it is σ 2 in the sub-Andes and σ 3 in the High Andes. This state of stress is in agreement with an effect of high topography such that the vertical principal stress σ zz, which is σ 3 in the lowlands, becomes σ 1 in the High Andes. However, in the Pacific Lowlands the state of stress at the surface is extensional and not compressional, as could be expected. An effect of warping of the continental plate along the convergence boundary or an effect of topography due to the nearby deep trench may be put forward. Therefore in high plateaus such as the Andes or Tibet, which are submitted to lateral compression, if extension is due to body forces, it should strike orthogonal to compression in the adjacent lowlands. In such a model, extensional direction may become parallel to the convergence direction only if boundary forces decrease drastically.

The state for stress in the Andean continental plate situated above the 30° dipping subduction appears to be different from that of the Andes of central Peru situated above the flat subducting segment. In a subsequent paper we shall report all the Quaternary and active faults observed in central Peru. These faults with available focal mechanisms will permit us to compare the different states of stress in the continental plate segments situated above slabs of different dips. This may improve our understanding concerning the control of the slab geometry and consequently of the asthenospheric wedge on the deformational regime in the upper continental plate.

APPENDIX

Using the approach of Bott (1959) and Price (1966), several authors (e.g., Carey and Brunier, 1974; Carey, 1976, 1979; Armijo and Cisternas, 1978; Angelier and Goguel, 1979; Etchecopar et al., 1981; Armijo et al., 1982; Angelier et al., 1982) have proposed quantitative computer-aided methods to interprete kinematics of faults in a highly fractured bodies of rocks.

The basic assumptions of all these numerical methods are (1) for a particular site a given tectonic event is characterized by a single homogeneous stress tensor, (2) for a given phase of deformation, if the material has an isotropic and homogeneous behavior, on each fault plane, slip (responsible for the striation) occurs in the direction and

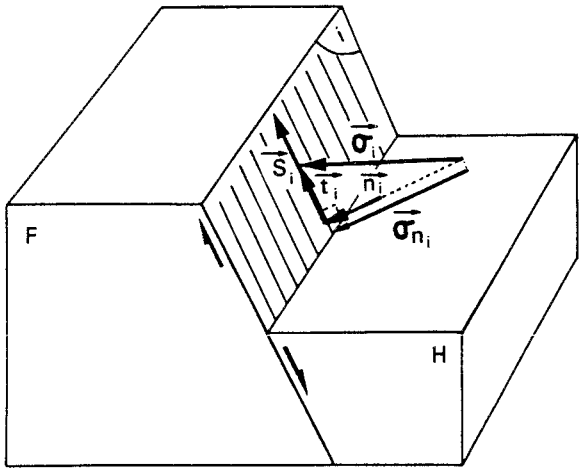

Fig. 20. Slip movement on a fault plane with parameters used in the Appendix (see text).

sense of the resolved shear stress acting on this fault plane, and (3) if there is no continuous deformation within the blocks separated by faults, if there is no fault plane rotation during deformation, and if the slips on the slickensides are independent and small respective to the fault length, deformation occurs as relative displacements of rigid blocks along the faults.

A state of stress is characterized by a stress tensor T which can be divided into an isotropic pressure tensor aI and in a deviatoric stress tensor bD, this latter being responsible for the resolved shear stress $\vec{t}$ which induces of the movements blocks. If the previous assumptions 1, 2, and 3 are satisfied, then the deviatoric stress tensor of a tectonic event can be obtained from, several independent striations related to this event, to within a multiplicative constant (Carey and Brunier, 1974; Carey, 1976).

For each measured striated slickensides (i) two vectors $\vec{ni}$ and $\vec{si}$ are defined (Figure 20); $\vec{ni}$ is the unit vector normal to the fault plane which has a downword component; $\vec{Si}$ is the unit vector which is oriented parallel to the movement of the footwall block (F) with respect to the hangingwall block (H). The stress $\vec{\sigma i}$ applied to a fault plane (i) is $\vec{\sigma i}=\vec{\sigma ni}+\vec{ti}$; oni corresponds to the stress component normal to the fault plane (i), the resolved shear stress $\vec{ti}$ is the projection of i on the fault plane (i) (see Figure 20).

The above-mentioned definitions imply that $(\vec{ti},\vec{Si})=0$; $\vec{ti}$ is a function of the four parameters which define the deviatoric stress tensor: the three Euler angles which give the azimuthal directions of the principal stress axes and the relative ratio (R) of principal stresses such as

$$R=(\sigma'2-\sigma'1)/(\sigma'3-\sigma'1)$$

with $\sigma'1 \quad \sigma'2 \quad \sigma'3$; $\sigma'1$ is the compressional deviatoric stress, $\sigma'2$ is the intermediate deviatoric stress, $\sigma'3$ is the tensional deviatoric stress. Furthermore, compressional stresses are noted negative and tensional ones positive.

The four parameters values must thus be in agreement with $(\vec{ti},\vec{Si})\longrightarrow 0$, and they are therefore determined when the function

$$F=-\sum_{i=1}^{N} ki*\cos^2(\vec{ti},\vec{Si})$$

is minimum, with N= number of fault planes measured, ki=-1 if $(\vec{ti},\vec{Si}) \geqslant 90°$, ki=1 if $(\vec{ti},\vec{Si}) < 90°$. More details on the minimization process can be obtained from Carey (1976, 1979).

Theoretically, the minimum of F might be equal to -N. Nevertheless, we consider the minimization to be mathematically good if all the $(\vec{ti},\vec{Si})$ are inferior to 20° or if this minimum is inferior to -90% of N. Anyway the minimum can be superior to -90% of N and the result considered as correct if 80% of the $(\vec{ti},\vec{Si})$ are inferior to 20° because the solution is stable, i.e., remains the same when only the 80% of the N data are used to calculate the deviatoric stress tensor. This limit permits us to take into account the errors of measurements and is justified by the fact that the variation of the $\cos^2(\vec{ti},\vec{Si})$ is low, being up to 20°. This simple mechanical model was applied to many field cases and provided a good interpretation in terms of stresses for the striations observed on the fault planes, especially when there is a single phase of deformation in a highly fractured body of rocks. More sophisticated calculations must be used to separate data corresponding to several tectonic phases (Carey, 1979; Etchecopar et al., 1981; Armijo et al.,1982).

Acknowledgments. Field work has been supported by Instituto Geofisico del Peru, ORSTOM Lima, and ATP Geodynamique II (Institut National d'Astronomie et de Géophysique). We are grateful to the Servicio Aerofotografico Nacional del Peru which authorized publication of aerial photographs. The authors thank C. Froidevaux, D. Hatzfeld and the two reviewers, B. Isacks and P. Tapponnier, for helpful comments and B. Purser for reading the English manuscript.

REFERENCES

Allmendiger, R. W., V. A. Ramos, T. E. Jordan, M. Palma, and B. L. Isacks, Paleogeography and Andean structural geometry, northwest Argentina, Tectonics, 2, 1-16, 1983.

Angelier, J., and J. Goguel, Sur une méthode simple de détermination des axes principaux des contraintes pour une population de failles, C. R. Hebd. Séances Acad. Sc., 288, 307-310, 1979.

Angelier, J., A. Tarantola, B. Valette, and S. Manoussis, Inversion of field data in fault tectonics to obtain the regional stress, 1, Single phase population: A new method of computing the stress tensor, Geophys. J. R. Astron. Soc., 69, 607-621, 1982.

Armijo, R., and A. Cisternas, Un problème inverse en microtectonique cassante, C. R. Hebd. Séances Acad. Sc., 287, 595-598, 1978.

Armijo, R., E. Carey, and A. Cisternas, The inverse problem in microtectonics and the separation of tectonic phases, Tectonophysics, 82, 145-160, 1982.

Armijo, R., P. Tapponnier, J. L. Mercier, and Han T., Quaternary extension of the Tibetan plateau: Field observations and tectonic implications, Paper presented at the International Symposium on Geology of the Himalayas, Chengdu, People's Republic of China, June 1984.

Aubouin, J., A. V. Borrello, G. Cecioni, R. Charrier, P. Chotin, J. Frutos, R. Thiele, and J. C. Vicente, Esquisse paléogéographique et structurale des Andes méridionales, Rev. Géogr. Phys. Géol. Dyn., 15(1-2), 11-72, 1973.

Audebaud, E., Geologia de los cuadrangulos de Ocongate y Sicuani, Bol. Ser. Geol. Min., 25, 72 pp., 1973.

Audebaud, E., R. Capdevila, B. Dalmayrac, J. Debelmas, G. Laubacher, C. Lefèvre, R. Marocco, C. Martinez, M. Mattauer, F. Mégard, J. Paredes, and P. Tomasi, Les traits géologiques essentiels des Andes centrales (Pérou-Bolivie), Rev. Géogr. Phys. Géol. Dyn., 15(1-2) 73-114, 1973.

Barazangi, M., and B. Isacks, Spatial distribution of earthquakes and of the Nazca plate beneath South America, Geology, 4,(11), 686-692, 1976.

Barazangi, M., and B. Isacks, Subduction of the Nazca plate beneath Peru: Evidence from spatial distribution of earthquakes, Geophys. J. R. Astron. Soc., 57, 537-555, 1979

Beaudet, G., D. Herm, R. Laharie, and R. Paskoff, Sur l'existence du Pliocène marin le long de la côte du Pérou, C. R. Somm. Séances Soc. Géol. Fr., 1, 12-13, 1976.

Bevis, M., and B. Isacks, Hypocentral trend surface analysis: Probing the geometry of Benioff zones, J. Geophys. Res., 89,(B7), 6153-6170, 1984.

Blanc, J. L., Etude néotectonique et sismotectonique des Andes du Pérou central dans la région de Huancayo, thesis, 158 pp., Univ. Paris-Sud, Orsay, 1984.

Blanc, J. L., J. Cabrera, and M. Sébrier, Estudio microtectonico de la falla sismica de Huaytapallana (Andes del Peru central), Rev. Geofisica Inst. Panam. Geogr. Hist., Mexico, 18/19, 5-24, 1983.

Bles, J. L., J. Goguel, A. Lavenu, P. Masure, Néotectonique et sismicité du site de La Paz (Bolivie): Un exemple de failles récentes sans trace de sismicité historique; conséquences pratiques pour le développement urbain, Bull. Bur. Rech. Géol. Min., Sect. 4, 2, 109-117, 1980.

Bonnot, D., Néotectonique et tectonique active de la Cordillère Blanche et du Callejon de Huaylas (Andes nord-péruviennes), thesis, 96 pp., Univ. Paris-Sud, Orsay, 1984.

Bott, M. H. P., The mechanics of oblique slip faulting, Geol. Mag., 97,(2), 109-117, 1959.

Cabrera, J., Etudes sur la néotectonique de la région de Cuzco: Zone Andine et zone Sub-Andine, sud Pérou, report Diplom. Etud. Approf., 55 pp., Univ. Paris-Sud, Orsay, 1984.

Carey, E., Analyse numérique d'un modèle mécanique élémentaire appliqué à l'étude d'une population de failles: Calcul d'un tenseur moyen des

contraintes à partir des stries de glissement, thesis, 138 pp., Univ. Paris-Sud, Orsay, 1976.

Carey E., Recherche des directions principales de contraintes associées au jeu d'une population de failles, Rev. Géogr. Phys. Géol. Dyn., 21,(1), 57-66, 1979.

Carey, E., and B. Brunier, Analyse théorique et numérique d'un modèle mécanique élémentaire appliqué à l'étude d'une population de failles, C. R. Hebd. Séances Acad. Sc., 279, 891-894, 1974.

Chinn, D. S., and B. L. Isacks, Accurate source depths and focal mechanisms of shallow earthquakes in western South America and in the New Hebrides Island Arc, Tectonics, 2(6), 529-563, 1983.

Clapperton, C., The Pleistocene moraine stages of west-central Peru, J. Glaciol., 11, 62, 255-263, 1972.

Cross, T. A., and R. H. Pilger, Controls of subduction geometry, location of magmatic arcs and tectonics of arc and back-arc regions, Geol. Soc. Am. Bull., 93, 545-562, 1982.

Dalmayrac, B., Un exemple de tectonique vivante: Les failles subactuelles du pied de la Cordillère Blanche (Pérou), Cah. ORSTOM, Sér. Géol., 6(1), 19-27, 1974.

Dalmayrac, B., and M. Mattauer, Subduction et phases de compression dans la chaîne des Andes, C. R. Hebd. Séances Acad. Sc., 209, 1345-1348, 1980.

Dalmayrac, B. and P. Molnar, Parallel thrust and normal faulting in Peru and constraints on the state of stress, Earth Planet. Sci. Lett., 55, 473-481, 1981.

Etchecopar, A., G. Vasseur, and M. Daignères, An inverse problem in microtectonics for the determination of stress tensors from fault striation analysis, J. Struct. Geol., 3(1), 51-65, 1981.

Fornari, M., G. Herail, and G. Laubacher, El oro en la Cordillera Suroriental del Peru: El placer fluvioglacial de San Antonio de Poto (departamento de Puno) y sus relaciones con la mineralizacion primaria de la Rinconada, in Proceedings V Congreso Latin American Geology-Argentina, vol. IV, pp. 369-386, Buenos Aires, 1982.

Froidevaux, C., and B. L. Isacks, The mechanical state of the Altiplano-Puna segment of the Andes, Earth Planet. Sci. Lett., 71, 305-314, 1984.

Grange, F., Etude sismotectonique détaillée de la subduction lithosphérique au Sud Pérou, thesis, 90 pp., Univ. Grenoble, Grenoble, France, 1983.

Grange, F., P. Cunningham, J. Gagnepain, D. Hatzfeld, P. Molnar, L. Ocola, A. Rodriguez, S. W. Roecker, J. M. Stock, and G. Suarez, The configuration of the seismic zone and the downgoing slab in southern Peru, Geophys. Res. Lett., 11(1), 38-41, 1984a.

Grange, F., D. Hatzfeld, P. Cunningham, P. Molnar, S. W. Roecker, G. Suarez, A. Rodriguez, and L. Ocola, Tectonic implications of the microearthquake seismicity and fault plane solutions in southern Peru, J. Geophys. Res., 89(B7), 6139-6152, 1984b.

Hasegawa, A., and I. S. Sacks, Subduction of the Nazca plate beneath Peru as determined from seismic observations, J. Geophys. Res., 86(B6), 4971-4980, 1981.

Huaman, D., Evolution tectonique cénozoique et néotectonique du Piemont Pacifique dans la région d'Arequipa (Andes du sud Pérou), thesis, 220 p., Univ. Paris-Sud, Orsay, 1985.

Heim, A., Observaciones geologicas en la region del terremoto de Ancash de Noviembre de 1946, Soc. Geol. Peru V. Jub., 2(6), 28 pp., 1949.

Isacks, B. L., and M. Barazangi, Geometry of Benioff zones: Lateral segmentation and downward bending of the subducted lithosphere, in Island Arcs, Deep Sea Trenches, and Back-Arc Basins, Maurice Ewing Ser., vol. 1, edited by M. Talwani and W. C. Pitman III, pp. 99-114, AGU, Washington, D. C., 1977.

Johnson, S. H., and G. E. Ness, Shallow structures of the Peru margin, Mem. Geol. Soc. Am., 154, 525-544, 1981.

Jordan, T. E., B. L. Isacks, R. W. Allmendiger, J. A. Brewer, V. A. Ramos, and C. J. Ando, Andean tectonics related to geometry of subducted Nazca plate, Geol. Soc. Am. Bull., 94(3), 341-361, 1983.

Laharie, R., Cronologia del Cuaternario Peruano, in Proceedings I Congreso Latin American Geology, vol. 6, pp. 145-157, Soc. Geol. Peru, Lima, 1970.

Laubacher, G., G. Herail, M. Fornari, and M. Sébrier, Le Piémont Amazonien des Andes Sud Orientales du Pérou (Marcapata-Inambari), paper presented at the Coll. Piemonts, Ass. Géol. S. O. Toulouse, France, 1982.

Lavenu, A., Néotectonique des sédiments plio-quaternaires du Nord de l'Altiplano bolivien (région de La Paz-Ayo Ayo-Umala), Cah. ORSTOM Sér. Géol., 10(1), 115-126, 1978.

Lavenu, A., Origine et évolution néotectonique du lac Titicaca, Rev. Hydrobiol. Trop., 14(4), 289-297, 1981.

Lavenu, A., and O. Ballivian, Estudios neotectonicos de las cuencas de las regiones de Cochabamba, Sucre, Tarija, Cordillera Oriental, Bolivia, Rev. Acad. Nac. Cienc. Bolivia, 2(3), 107-129, 1980.

Lavenu, A., and J. P. Soulas, Observacion de microfallas Plio-Cuaternarias en distension a lo largo de la costa sur del Peru, Bol. Soc. Geol. Peru, 52, 39-48, 1976.

Lavenu, A., M. Sébrier, and M. Servant, Néotectonique des Andes Centrales: Pérou, Bolivie, Bull., 3, pp. 56-58, INQUA Neotectonic Comm., Stockholm, 1980.

Lavenu, A., M. Fornari, and M. Sébrier, Existence de deux nouveaux épisodes lacustres quaternaires dans l'Altiplano péruvo-bolivien, Cah. ORSTOM Sér. Géol., 14(1), 103-114, 1984.

Lefèvre, C., Les caractères magmatiques du volcanisme plio-quaternaire des Andes dans le Sud du Pérou, Contrib. Mineral. Petrol., 41, 259-272, 1973.

Legault, R. Z., Preliminary study of marine terraces in the Marcona-San Juan area of southern Peru, report, Marcona Mining Co, Hierroperu Marcona, 1963.

Lettau, H. H., and K. Lettau, Exploring the world's driest climate, Rep. 101, pp. 1-26, Inst. for Environ. Stud., Univ. Wisc., Madison, 1978.

Macharé, J., Geologia del Cuaternario en la costa del Peru central, thesis, 197 pp., Univ. Nac. Ing., Lima, 1981.

Malgrange, M., A. Deschamps, and R. Madariaga, Thrust and extensional fauting under the Chilean coast: 1965, 1971 Aconcagua earthquakes, Geophys. J. R. Astron. Soc., 66, 313-331, 1981.

Martinez, C., Structure et évolution de la chaîne Hercynienne et de la chaîne Andine dans le nord de la cordillère des Andes de Bolivie, Trav. Doc. ORSTOM, 119, 352 pp., 1980.

Mégard, F., and H. Philip, Plio-Quaternary tectono-magmatic zonation and plate tectonics in the Central Andes, Earth Planet. Sci. Lett., 33, 231-238, 1976.

Mégard, F., D. C. Noble, E. McKee, and H. Bellon, Multiple pulses of Neogene deformation in the Ayacucho intermontane basin, Andes of central Peru, Geol. Soc. Am. Bull., 95(9), 1108-1117, 1984.

Mercer, J. H., and O. Palacios, Radiocarbon dating of the last glaciation in Peru, Geology, 5, 600-604, 1977.

Mercier, J. L., Extensional-compressional tectonics associated with the Aegean Arc: Comparison with the Andean Cordillera of south Peru-north Bolivia, Philos. Trans. R. Soc. London, Ser. A, 300, 337-355, 1981.

Mercier, J. L., and M. Sébrier, Informe sobre el estudio preliminar de las fallas recientes de la region de la represa de Recreta (Cordillera Blanca, Dep. Ancash), report, 8 pp., Electroperu, Lima, 1981.

Mercier, J. L., N. Delibassis, A. Gauthier, J. J. Jarrige, F. Lemeille, H. Philip, M. Sébrier, and D. Sorel, La néotectonique de l'Arc Egéen, Rev. Géogr. Phys. Géol. Dyn., 21(1), 67-92, 1979.

Mercier, J. L., P. Tapponnier, R. Armijo, E. Carey-Gailhardis, Han T., and Zhou J., Folding, kinematics of faults and evolution of the state of stress in southern Tibet, paper presented at the International Symposium on Geology of the Himalayas, Chengdu, People's Republic of China, June 1984.

Minster, J. B., and T. H. Jordan, Present-day plate motions, J. Geophys. Res., 83, 5331-5334, 1978.

Minster, J. B., T. H. Jordan, P. Molnar, and E. Haines, Numerical modelling of instantaneous plate tectonics, Geophys. J. R. Astron. Soc., 36, 541-576, 1974.

Molnar, P., and P. Tapponnier, Active tectonics of Tibet, J. Geophys. Res., 83, 5351-5375, 1978.

Nakamura, K., and S. Uyeda, Stress gradient in arc-back arc regions and plate subduction, J. Geophys. Res., 85(B11), 6419-6428, 1980.

Price, N. J., Fault and Joint Development in Brittle and Semi-Brittle Rock, Pergamon, New York, 1966.

Sacks, I. S., A. T. Linde, A. Rodriguez, and J. A. Snoke, Shalow seismicity in subduction zones, Geophys. Res. Lett., 5(11), 901-903, 1978.

Schweller, W. J., L. D. Kulm, and R. A. Prince, Tectonics, structure and sedimentary framework of the Peru-Chile Trench, Mem. Geol. Soc. Am., 154, 323-350, 1981.

Sébrier, M., and C. de Muizon, Comporte-

ment Plio-Pléistocène de la côte péruvienne au niveau de la déflection de Pisco (Andes centrales), IX Réun. Ann. Sc. Terre, p. 575, Paris, 1982.

Sébrier, M., and J. Machare, Observaciones acerca del Cuaternario de la Costa del Peru central, Bull. Inst. Fr. Etud. Andines, 9(1-2), 5-22, 1980.

Sébrier, M., R. Marocco, J. J. Gross, S. Macedo, and M. Montoya, Evolucion neogena del Piedemonte Pacifico de los Andes del Sur del Peru, in Proceeding II Congreso Geology Chile, vol. 3, p. 71-88, Inst. Invest. Geol., Arica, 1979.

Sébrier, M., G. Laubacher, R. Marocco, A. Lavenu, and M. Servant, Evolution tectonique Cénozoïque des Andes Centrales (Sud Pérou-Bolivie), paper presented at the 26th International Geological Congress, Soc. Géol. Fr., Paris, 1980a.

Sébrier, M., A. Lavenu, and M. Servant, Apuntes recientes sobre la neotectonica en los Andes Centrales (Peru-Bolivia), Bull. Inst. Fr. Etud. Andines, 9(1-2), 1-3, 1980b.

Sébrier, M., D. Huaman, J. L. Blanc, J. Macharé, D. Bonnot, and J. Cabrera, Observaciones acerca de la Neotectonica del Peru, 109 pp., Inst. Geofisico Peru, Seismicity Seismic Risk Andin Region, Lima, 1982.

Servant, M., Le cadre stratigraphique du Plio-Quaternaire de l'Altiplano des Andes tropicales de Bolivie, Rech. Fr. INQUA, suppl., Bull. Ass. Fr. Etud. Quat., 1(50), 323-327, 1977.

Silgado, E., The Ancash, Peru, earthquake of November 10, 1946, Bull. Seismol. Soc. Am., 41, 83-100, 1951.

Silgado, E., Historia de los sismos mas notables ocurridos en el Peru (1513-1974), Bol. 3, Ser. C, 130 pp., Inst. Geol. Min., Lima, 1978.

Soulas, J. P., Tectonique quaternaire: La côte pacifique et la chaîne andine du Pérou central, Rev. Géogr. Phys. Géol. Dyn., 20(5), 399-414, 1978.

Stauder, W., Mechanism and spatial distribution of Chilean earthquakes with relation to subduction of the oceanic plate, J. Geophys. Res., 73(23), 5033-5061, 1973.

Stauder, W., Subduction of the Nazca plate under Peru as evidence by focal mechanisms and by seismicity, J. Geophys. Res., 80(8), 1053-1064, 1975.

Suarez, G., P. Molnar, and B. C. Burchfiel, Seismicity, fault plane solutions, depth of faulting, and active tectonics of the Andes of Peru, Ecuador, and southern Colombia, J. Geophys. Res., 88(B12), 10403-10428, 1983.

Tapponnier, P., and P. Molnar, Slip-line field theory and large-scale continental tectonics, Nature, 264, 319-324, 1976.

Tapponnier, P., and P. Molnar, Active faulting and Cenozoic tectonics of the Tien Shan, Mongolia, and Baikal regions, J. Geolphys. Res., 84, 3245-3459, 1979.

Tapponnier, P., J. L. Mercier, R. Armijo, Han T., and Zhou J., Field evidence for active normal faulting in Tibet, Nature, 294, 410-414, 1981.

Uyeda, S., Subduction zones and back arc basins: A review, Geol. Rundsch., 70(2), 552-569, 1981.

Uyeda, S., Subduction zones: An introduction to comparative subductology, Tectonophysics, 81, 133-159, 1982.

Uyeda, S., and H. Kanamori, Back arc opening and the mode of subduction, J. Geophys. Res., 84, 1049-1061, 1979.

Vicente, J. C., F. Sequeiros, M. A. Valdivia, and J. Zavala, El cabalgamiento de Cincha-Pampacolca: Elemento del acidente mayor andino al NW de Arequipa (Sur del Peru), Bol. Soc. Geol. Peru, 61, 67-99, 1979.

Yonekura, N., T. Matsuda, M. Nogami, and S. Kaizuka, An active fault along the western foot of the Cordillera Blanca, Peru, Chigaku Zasshi, 88(1), 1-19, 1979.

E. Carey-Gailhardis, J. L. Mercier, and M. Sébrier, Laboratoire de Géologie Dynamique Interne, U.A. 730 CNRS, bat. 509, Université Paris-Sud, 91405 Orsay cedex, France.

G. Laubacher, ORSTOM, 24 rue Bayard, 75008 Paris, France.

F. Mégard, Centre Géologique et Géophysique, Université des Sciences et Techniques du Languedoc, 34060 Montpellier, France.

(Received January 17, 1985;
revised June 21, 1985;
accepted June 23, 1985.)